

Received April 10, 2019, accepted May 20, 2019, date of publication May 27, 2019, date of current version June 11, 2019.

Digital Object Identifier 10.1109/ACCESS.2019.2919324

# Communication Technologies Based on Voluntary Blinks: Assessment and Design

ALBERTO J. MOLINA-CANTERO<sup>1</sup>, CLARA LEBRATO-VÁZQUEZ, MANUEL MERINO-MONGE, ROYLÁN QUESADA-TABARES, JUAN A. CASTRO-GARCÍA, (Student, IEEE), AND ISABEL M. GÓMEZ-GONZÁLEZ, (Senior Member, IEEE)

Department of Electronic Technology, E.T.S. Ingeniería Informática, Universidad de Sevilla, 41012 Seville, Spain

Corresponding author: Alberto J. Molina-Cantero (almolina@us.es)

**ABSTRACT** Some people with severe disabilities are confined in a state in which communication is virtually impossible, being reduced to communicating with their eyes or using sophisticated systems that translate thoughts into words. The EyeTrackers and Brain-Computer Interfaces (BCIs) are suitable systems for those people but their main drawback is their cost. More affordable devices are capable of detecting voluntary blinks and translating them into a binary signal that allows the selection, for example, of an ideogram on a communication board. We tested four different systems based on infrared, bioelectrical signals (Electro-Oculography (EOG) and Electro-Encephalography (EEG)), and video processing. The experiments were performed by people with/without disabilities and analyzed the systems' performances, usability, and method of voluntary blinking (long blinks or sequence of two short blinks). The best accuracy (99.3%) was obtained using Infrared-Oculography (IR-OG) and the worst with the EEG headset (85.9%) and there was a statistical influence of the technology on accuracy. Regarding the method of voluntary blinking, the use of long or double blinks had no statistical influence on accuracy, excluding EOG, and the time taken to perform double blinks was shorter, resulting in a potentially much faster interface. People with disabilities obtained similar values but with greater variability. The preferred technology and blinking methods were Video-Oculography (VOG) and long blinks, respectively. The several Open-Source Hardware (OSHW) devices have been developed and a new algorithm for detecting voluntary blinks has also been proposed, which outperforms most of the published papers in the reviewed literature.

**INDEX TERMS** AAC, blinks, EEG, EOG, IROG, people with disabilities, VOG.

## I. INTRODUCTION

To develop our everyday activities we have to interact with the environment using our communicative abilities (oral, written or gestural). People with severe disabilities have great difficulty completing this interaction. Fortunately, Augmentative and Alternative Communication (AAC) technologies have promoted the integration of this group of people by converting their capabilities into a communicative action.

Some AAC devices rely on transforming users' intentions into commands sent to a computer. For people with severe disabilities, the most typical computer interaction is by means of a device that generates a binary on/off signal, to select a highlighted ideogram during

the scanning of the elements contained on a communication board. The physicist Stephen Hawking, for example, controlled a scanning-based communication program (ACAT) <https://github.com/intel/acet/releases> via his cheek movements detected by an Infrared (IR)-based device placed on his spectacles.

Several diseases, like Amyotrophic Lateral Sclerosis (ALS), Locked-in Syndrome (LIS), etc., confine people to a state in which it makes it hard for them to perform the simplest movement. Stephen Hawking suffered from ALS [98], a neurodegenerative disease, also called Lou Gehrig's disease, that gradually kills off motor neurons leading to a progressive loss of muscular control. This results in difficulty speaking, swallowing and eventually breathing; however voluntary eye movements remain unaffected throughout the disease. Only if the disease course is prolonged via mechanical ventilation, individual case reports

show that the oculomotor muscles might also be weakened, producing ophthalmoplegia, nystagmus or slowing of saccades [72].

LIS is caused by a severe damage affecting the pons and can be provoked by an infarct, hemorrhage or trauma, causing quadriplegia, lower cranial nerve paralysis and mutism, but with preservation of only vertical gaze and upper eyelid movement in a conscious patient [5]. LIS has been classified into three categories: *Classic*, quadriplegia and anarthria with consciousness and vertical eye movements; *Incomplete*, the same as classic but with preservation of more voluntary movements; *Total*, total immobility and inability to communicate with full consciousness [82]. Other diseases, such as some variants of Cerebral Palsy (CP), quadriplegia or muscular dystrophy leave subjects with very limited capacity to perform any kind of movement apart from blinking or eye gazing.

Several AAC solutions exist to facilitate communication in these cases [19]. Eye-Tracker Interfaces (ETI) can be used by people with good eye gaze control [30]. Most of these are based on the reflection of an IR light on the surface of the eye. A camera tracks the pupil and the shiny IR spot in the eye. The relative position between them serves to determine the eye gaze after an initial calibration process. The main drawback with technology is the cost [81] and the so-called Midas' touch effect [90] which consists of the random selection of an icon on the computer screen followed by the user's gaze. This is a problem when the user is not sure of the icon's meaning and requires a longer time to understand and mentally process the action related to it. Several low-cost and open-source solutions have emerged for eye tracking (see [http://wiki.cogain.org/index.php/Eye\\_Trackers](http://wiki.cogain.org/index.php/Eye_Trackers) for a review) with positioning accuracy similar to the proprietary counterparts [12], [63]. Furthermore, some eye trackers, using only on a webcam, have shown that the accuracy obtained is similar to IR devices when reasonably sized images are used and the periphery of the screen is avoided [8].

BCI is another plausible solution that does not need precise control over eye muscles. There are several modalities of BCI [61] depending on how brain activity is measured, the type of information extracted and the nature of the stimuli. The scientific literature includes plenty of BCI systems measuring electrical cortical activity through electrodes placed on the scalp. There are several types of BCI. Amongst which we would like to highlight: Slow cortical potential (SCP), Motor Imagery (MI), Steady state visual potential (SSVEP) and P300. SSVEP and P300 are evoked potentials that differ from the other two in that an external stimulus is necessary. The stimulus in SSVEP is visual whereas in P300 it can be visual, auditory or tactile. The main drawback with this technology is the cost of the equipment, the training time for some BCI modalities and the technical knowledge needed by the caregivers to setup the system. Nevertheless, inexpensive BCI, such as NeuroSky Mindwave (NM), Muse and Emotiv, have recently been released. The first is the cheapest, with one electrode, followed by Muse, with 4 channels and, finally,

Emotiv with up to 14 channels. Previous works have shown the efficacy of using NM as computer access method, by modulating the level of users' attention [54], or for detecting a reduced number of emotions [71]. In [13], NM and Emotiv were compared to detect cognitive loads. The authors found that Emotiv gave better results but recognized the advantages of MindSet because it is more user-friendly, easier to setup and maintain.

Other BCI interfaces are based on the hemodynamic response rather than the firing activity of the cortical neurons. Near Infrared Spectroscopy (NIRS) is a relatively new BCI modality [79] that measures such a response. As the hemodynamic is temporally delayed from the onset of the underlying electric neural activity, the response is expected to appear with a latency of several seconds after any change in participants' behavioral or mental states. This could severely limit the practical use of such systems.

The Information Transfer Rate (ITR) [47], [96] was introduced to compare the throughput for different BCI systems. ITR is based on the Shannon's classic Information Theory, and measures the capacity of a BCI channel in bits/min. It depends on the number of choices, the accuracy of the classifier in detecting them and the time taken to make a classification. According to [61], the NIRS has an ITR of around 4 bits/min while its electrical counterparts obtained better results. For SCP, MI and P300, the ITR was 5–12 bits/min, 3–35 bits/min and 20–25 respectively. The highest score was achieved by SSVEP that reached a bit rate between 60–100 bits/min.

ETI and P300 interfaces were compared in [66]. Results showed that ITR and usability of the eye tracker were higher than the P300 which also showed higher cognitive workload. A more recent study [85] demonstrated that an SSVEP BCI obtained results comparable to the ETI in terms of accuracy and ITR. In particular, when the size of a target was relatively small, the BCI performed significantly than the ETI. Although the BCI approach is usually more tiring for users, it remains an option for by people in locked-in state once control over eye muscles is no longer possible [32].

Communication with eyes, by using voluntary blinking as a binary signal, is the way that some people have been able to communicate. In a study performed in collaboration with the French Association of Locked-in syndrome (ALIS) [40] 88 respondents reported using a yes/no communication code using mainly eye movements. The case of the French journalist and writer Jean-Dominique Bauby is also noteworthy. He wrote *'The Diving Bell and the Butterfly'* solely by means of blinks, after suffering a stroke that left him with LIS. The book took 200,000 blinks and ten months to write at an average of 0.5 Words per Minute (WPM).

Cheaper devices for detecting voluntary eye gestures can be built based on IR diodes placed on spectacles, or by processing the video signal recorded by a simple webcam or through bioelectrical signals captured with electrodes placed around the eye [68]. For those systems, it is not usual to find their ITR in the scientific literature, but its estimation

is required to establish a comparison with other technologies. To do that, the accuracy and length of the temporal window used to obtain the classifier output are needed. As an example, in [36] the authors presented an image processing system with an accuracy of 95% when using processing windows of 2s. For that system, the ITR was of 21.5 bits/min, placing it in the range of P300 BCI systems. Other more common indicators, such as WPM, can be used to compare system performances. Remarkable results were obtained in [42], where the authors developed a method for typewriting managed by voluntary blinks, filtering the involuntary ones through temporal constraints, and using an ambiguous virtual keyboard with word prediction. They obtained a WPM rate of 4.58 WPM with an error rate of 1.02% using a scanning period of 850 ms. This outperforms the results with other technologies based on Electro-Myography (EMG), non-verbal vocal interaction, push buttons, EEG and gaze interaction found in several scientific reports mentioned in [69] and places it in the range of some eye trackers [74]. The examples above show that it is worth considering the use of voluntary blinking detection technology as a feasible option for AAC.

There will always be an optimal solution from several possibilities, for each personal situation, as far as ITR or other technical parameters are concerned, but in the end, the opinion of the users is the key to accepting a specific technology. This is because other non technical aspects such as fatigue, price, frustration, training time, environment, etc are also taken into account [22]. Authors in [32] demonstrated that a person in LIS was able to gain control over an EOG, an eye tracker and an auditory BCI, but the user preferred to keep on employing his low-tech communication method, using residual eye movements, due to the user's and his caregivers' proficiency in using it. Finally, we would like to show some of Stephen Hawking's words, related to this topic and collected from the website <http://www.hawking.org.uk/the-computer.html>, about the reasons for using his AAC system: *'I keep looking into new assistive technologies, and I have experimented with eye tracking and brain controlled interfaces to communicate with my computer. However although they work well for other people, I still find my cheek operated switch easier and less fatiguing to use.'*

In this work, we have assessed inexpensive devices (< \$100), developed new low-cost OSHW platforms and collected the opinion of users after interacting a computer with technologies that detect voluntary blinks. Section II shows the state of the art, section III outlines the devices used in the experiments, Sections V and VI show the procedures followed for collecting data and the results, and, finally, Sections VII and VIII include the discussion and conclusions respectively.

## II. STATE OF THE ART

This section contains a literature review about different techniques employed to detect blinking.

### A. IR-OG

Infrared-based technologies are cheap and easy to set up. Several designs can be found in the scientific literature. The simplest one is based on one emitter diode and one receiver phototransistor that can be placed at different positions: a) both emitter/receiver facing the eye, in the same container, measuring changes in the reflected IR beam when the eye is covered by the eyelid [57], [58], [73]; b) both emitter/receiver aside the eye, in the same container, and based on measuring the IR reflected by the cornea/eyelid [9], [14], [64]; c) photodiode and phototransistor on both sides of the eye, facing one another, so that the IR beam runs along the cornea towards the receptor if the eye is open, and interrupted or blocked when it is closed [20]. More complex designs include multiple photo-diodes, -transistors arranged around the eye to improve eye-gesture detection [55] or increase the number of user actions [10]. The IR elements can be powered by a Direct Current (DC) supply voltage or by a pulsed supply voltage that turns them on/off periodically. The latter makes the sensor less sensitive to the ambient IR level, by amplifying the difference in the received IR radiation between periods of activation/inactivation [55], [73].

In most cases the IR elements are mounted on spectacle frames, but more sophisticated structures can also be found, such as that used to study blink conditioning in free-living animals. They required surgery to cement the sensor support to their skulls [94].

IR-OG has been employed as a method of AAC for people with disabilities by filtering natural blinking and converting voluntary blinks into computer events such as mouse clicks [44], [64] or a communication code (e.g. Morse) [57]. The AAC methods described above are all based on single emitter-receiver IR montages placed near one eye. By increasing the number of emitters/receivers, and including both eyes, more ocular gestures, apart from blinking, can be detected. These gestures may include horizontal and vertical eye movements, left and right winks, sequences or combinations of them. The higher the number of detected gestures, the higher the speed of the communication rate of the AAC system.

Other applications uses this technology to guide powered wheelchairs [10], gauge driver drowsiness [58], promote symmetrical blinking in people with facial paralysis [20] or alleviate dry eyes in computer vision syndrome [14]. It is also used as an effective method for minimizing the number of wires when investigating conditioned blink reflex in animals [94], etc.

A final topic concerns the safety of this technology when used for long periods [9], [35]. There are several eye pathologies related to infrared and other exposed radiation wavelengths. In the range between (780 - 1400 nm) cataracts and retinal or skin burns may occur. In the case of a point-type and diverging beam source, such as Light Emitting Diode (LED), the hazard increases as the distance between the beam source and the eye shortens, providing that such a distance is greater

than the shortest focal length. Otherwise, there is a rapid growth of the retinal image and a corresponding reduction of irradiance, even though more power may be collected. The International Commission of Non-Ionizing Radiation Protection (ICNIRP) norm regarding thermal lesions for cornea and lens states that the ocular exposure should not exceed  $10 \text{ mWcm}^{-2}$  for lengthy exposures ( $> 1000 \text{ sec}$ ).

Table 1 summarizes the most important features of the reviewed literature. Most IR designs are based on mounting 1 channel containing 1 emitter/receiver on the glasses frame and using the reflected radiation to measure blinking. Two papers show the schematics of the implemented circuit [73], [94], so they can be considered as OSHW. The best accuracy in detecting blinking, 85%, was obtained by [14]. In [20] a 100% of sensitivity was achieved by pulse-powered emitters during experiments where subjects had to keep a forward gaze, although the results worsened with other gestures or gaze direction changes. Only one author included people with disabilities in the experiment [64], using a commercial equipment, with an accuracy of 70%.

## B. EOG

The EOG signal is derived from the polarization potential, also known as the Corneal-Retinal Potential (CRP), generated within the eyeball by the metabolically active retinal epithelium [91]. The electrical activity associated to eye movements can be measured by placing electrodes on the surface of the skin around the eye [21]. When the eyes are looking straightforward, the position of the cornea and retina makes the electrodes measure a steady electric field. If the eyes move towards the periphery, the retina approaches one electrode whereas the cornea approaches the other. This changes the orientation of the dipole and results in a variation in the measured EOG signal [23].

Typically, EOG amplitudes range between 0.05 and 3mV with a frequency bandwidth from DC to 50Hz [33]. At least three electrodes, with one acting as reference, are necessary to capture the signal. The EOG signal may also contain noise of no interest, mainly coming from the power line or from the electrical activity of the muscles near the eye. To suppress the former, a notch filter tuned to the power line frequency (50Hz or 60Hz) is usually applied. To reduce the influence of the latter, a bandpass filter with a frequency range between roughly 1Hz and 50Hz can be applied.

One important application for EOG is as an AAC system [27] for people with disabilities. Others include, for example, the control of multi-task gadgets through voluntary eye movements [21], biometric human identification and verification through blinking [1], wheelchair control [39], the classification of sleep/wake stages [100] or the identification of fatigue in changes in spontaneous eye blink rate [43].

Table 2 summarizes the most important features found in the reviewed literature. One aspect is the number of electrodes, related, in some extent, to the amount of single eye gestures that may be detected and the computational complexity. For example, with only two electrodes placed at the

same vertical line of one eye, it is only possible to detect blinks or eye gestures such as looking upwards or downwards. With more electrodes, placed vertically in both eyes for example, it would also be possible to recognize left and right winks; with horizontally distributed electrodes, rightward and leftward gazes; and with them all, any eye gesture combination such as for instance: firstly looking upwards, then rightwards and finally closing the eyes. The most frequent number of electrodes used in the reviewed studies is three or five, although it is possible to find some studies with higher amounts. The best accuracy shown in Table 2 is of 95.6% observed in [60] and referring only to the blink detection. In other articles, the value of accuracy has been calculated for other gestures and not especially for blinking. A final aspect to highlight is that most platforms used in experiments are not Open-Source Hardware OSHW.

## C. VOG

As mentioned in the introduction, ETI's are especially appropriate for people with good control over ocular movements. They are mainly based on employing specific cameras according to the type of scene illumination: IR or natural. Some eye-tracking open-source hardware uses a small camera, which is placed close to the eye (the *eye camera*), capturing eye movements accurately [65], [74]. This scheme is very sensitive to head movements and needs frequent calibrations to correct the loss in accuracy. Other solutions have included a second camera, or *field camera*, which records the scene that the subject sees, and allows the software to correct the eye-gaze according to the head position [31], [38], [63]. Other eye-trackers employ a Kinect [93], or a single webcam placed in front of the user, and do not need any additional mounting [80]. The webcam-based ETI can achieve an accuracy similar to the infrared counterparts when it uses reasonably sized images and avoids the periphery of the screen [8].

Whatever the type of hardware, the ETI software tracks the iris to evaluate the eye gaze and move the cursor to the position on screen the user is looking at [76]. There is plenty of literature on algorithms to detect eye gaze with an accuracy that, in most cases, is  $< 1^\circ$ . Once the cursor is placed on the desired element on the screen, it can be selected by keeping it still for a period of time. This method may cause the involuntary selection of an element on screen if a given subject is focused on it for long and for different reasons from the selection itself. This is the so-called Midas touch effect [90]. To prevent this, some ETI software has also included alternative selection methods such as, for example, that based on the detection of voluntary blinks [7], [65]. Although it is not common for ETI literature to include procedures for detecting voluntary blinks, several studies, in the area of image processing, have described algorithms for that purpose. Applications, such as the detection of driver drowsiness [2], for preventing Computer Vision Syndrome (CVS) [15], [26] or accessing a computer [36], have promoted research in that area.

**TABLE 1.** Summary of the main features in several IR-OG studies. Some acronyms used in the table: OSHW, International Commission of Non-Ionizing Radiation Protection (ICNIRP), Sensors Placed Aside the Eye (Sensor Aside Eye), Sensors Placed Facing the Eye (Sensor Facing Eye), Systems based on the Corneal reflection of the IR beam (Corneal Reflection), Systems based on Blocking the IR beam (Blocking IR beam).

Citation	AAC?	#Subjects	Montage	Hardware	OSHW?	Fulfills		Comment
						ICNIRP?	Accuracy	
Dementyev et al. [14]	No	12	Sensor Aside Eye Corneal Reflection On glasses frame	1 ch. 1 ER/ch	No	NA	85%	Alleviating dry eye. Puff actuator and flash included IR power radiation <20mW
Frigerio et al.[20]	No	24	Sensor Aside Eye Blocking IR beam On safety glasses	1 ch. 1 ER/ch Pulsed powered	No	Yes	NA	100% sensitivity in forward gaze based on amplitude difference. 87% correct detection based on signal derivative Detection results studied for face gestures and eye gaze directions
Lo Castro [9]	No	NA	Sensor Aside Eye Corneal Reflection	1 ch. 1 ER/ch Pulse powered	NA	Yes	NA	
Molina et al.[55]	Yes	NA	Sensor Facing Eye Corneal Reflection On glasses frame	2 ch. 4 ER/ch Pulse powered	No	NA	NA	Based on signal derivative and timers Detect eye gestures: up, down left, right, short-, long- blinks...
Mukherjee et al.[57]	Yes	NA	Sensor Facing Eye Corneal Reflection On glasses frame	1 ch. 1 ER/ch DC powered	Yes	NA	NA	Natural blinking filtered by timers. Communication provided via Morse codification
Park et al.[64]	Yes	1 (LIS)	Sensor Aside Eye Corneal Reflection On glasses frame	1 ch. 1 ER/ch	No	NA	70%	Weak blinks filtered out. Only strong ones detected. SCATIR Switch Interface Pro. Costs >\$800
Ryan et al. [73]	No	NA	Sensor Facing Eye Corneal Reflection	1 ch. 1 ER/ch Pulse powered	Yes	Yes	NA	Study of blink reflex in rabbits
Weiss et al.[94]	No	NA	Sensor Facing Eye Corneal Reflection Support cemented on skull	1 ch. 1 ER/ch DC powered	Yes	NA	NA	Study of blink reflex in free moving rats Puff actuator to force blinking

**TABLE 2.** Summary of the main features obtained from several EOG studies. Band pass filtering (BPF), Common Spatial Pattern (CSP), Electro-Oculography (EOG), Empirical Mean Curve Decomposition (EMCD), Horizontal peak amplitude (HPA), Infinite Impulse Response (IIR), Mathematical morphology (MM), Movement Classifier Deterministic Finite Automata (MCDFA), Neural Network classifier (NNC), Not available (NA), Peak Detection Deterministic Finite Automata (PDDFA), Principal Component Analysis (PCA), Sallen-Key filters (SKF), Savitzky-Golay (SVG), Support Vector Machine (SVM), Vertical peak amplitude (VPA), hardware description language (VHDL).

Citation	AAC?	#Subjects	OSHW?	#Electrodes	Methods	Accuracy	Comment
Gandhi et al[21]	Yes	10	No	5 H1 H2 V1 V2 GND(forehead)	BPF and logical circuit. Use VHDL to discriminate 128 different EOG states	95.33%	PDDFA, used as input by MCDFA. Recognizes 4 eye movements (up, down, left and right).
Mulam et al. [59]	No	NA	No	5 H1 H2 V1 V2 GND(forehead)	EMCD,PCA, NNC	78% (only blink)	Statistical procedure for the dimensional reduction of the EOG signal Recognizes 5 eye gestures
Hori et al[29]	Yes	5	No	3 A1 H1 Reference(earlobe)	BPF ( 0.53- 5Hz) Threshold Determination	94.16%	Outputs five kinds of intentions (up, down, left, right and wink).
Masaki et al[60]	No	8	No	6 V1 V2 H1 H2 Reference(mastoid) GND(forehead)	IIR (0.53- 15Hz), VPA, HPA, cross correlation between vertical EOG signals and template signal	95.56% (only blink)	SVM Recognizes 3 eye gestures
He et al[27]	Yes	8	No	3 V1, REF (R-mastoid) GND (forehead)	1.2s window length BPF (0.1-30 Hz). Energy, peak and valley difference SVM	94.13% (only blink)	
Guo et al[25]	Yes	8	No	3 V1 GND, REF (forehead)	1-s window length Smoothing SVG filter at 33.7Hz Signal peak and trough	83.3% (only blink)	Patch with 3 electrodes over the eyebrow. Three actions: blink, upward and downward
Zhao et al. [41]	Yes	10	No	10 H1 H2 V1 V2 A1 A2 A3 A4 GND, REF (mastoid)	32-order BPF (0.5-10Hz) Hamming window CSP, Kurtosis and energy	96.8%	Recognizes 8 eye gestures (up, down, left, right, right-up, left-up,right-down and left-down).
Zheng et al[99]	Yes	NA	Yes	5 H1 H2 V1 V2 GND(forehead)	EOG signals are sampled at the rate of 250 Hz. BPF (0.01-41Hz) is provided with two SKF	above 80%	Based on the MM, differential and integral algorithms.Detect up/down, left/right movement and voluntary eye blinking

The detection of eye blink, in many image processing methods, consists of two main steps: 1) to find the head and, then, the eye positions and 2) recognize if they are open or closed. For the first step, one of the most widely used algorithms is the Viola-Jones object detector [92], based on Haar-like features and an *AdaBoost* learning algorithm, which selects the best features and trains the classifier. Alternatively, in [56] authors employed a method for head detection based on measuring the difference among several video frames. The head area is around the center of mass of the thresholded images.

Once the head is detected, the eyes region is mainly located by applying, again, a) the Viola-Jones algorithm [16], [50], [51]; b) by computing the difference between video frames [24], [37], [77], c) by using variance maps [56], d) by applying geometrical rules [36] or e) by using previous knowledge acquired from databases [4]. Other works search for the direct detection of the eyes without having to find previously the head in the image. Assuming that the head is quite still among frames, the area that shows more variability is the ocular region due to blinking. In [24], [49] authors searched for difference among frames. This difference is related to the velocity of eye closure/opening. Another procedure is to locate the eye area by looking for specific patterns in the image. Namely, the area containing the eyes shows one vertically and two horizontally distributed valleys [37]. Some invariant features are found by applying Scale-Invariant Feature Transform (SIFT) which computes the difference between frames in the area of interest, resulting in a thresholded image of the blinking eye. A BackProjection method based on Hue-Saturation or Saturation Histograms has been used to obtain thresholded images in the eye area [70]. Some techniques like Continuously Adaptive MeanShift (CAMshift), isophote curvature [88] or the Lucas-Kanade (LK) method are applied for head/eye tracking [4], [56], [70].

The eye blink can be detected using different techniques. The most widely used compares the eye image with previously stored templates of open/closed eyes [11], [24], [36], [49], [77]. The correlation coefficient, between the current image and the templates, marks the blink occurrence. Other authors have based the detection on counting the number of pixels of binary images in the eye area. These thresholded images can be obtained in different ways. In [51], authors assumed that the histogram of a binary eye image changes with the eyelid position. In [16], [56], variance maps, which are affected by the blinking, were employed. The study in [70] thresholded an eye image using BackProjection of Hue-Saturation histograms. In [50], the authors converted the color image from the RGB to the YCbCr space. Thus, the cumulative histogram of the Y dimension was thresholded, which changes as the eyelid is close or open. Another option is shown in [83], where authors measured the eye aspect ratio (EAR) (by computing the height and width of the eye) from the results of two landmark detectors

(*Chehra* [3] and *Intraface* [97]) and a Support Vector Machine (SVM) classifier.

Table 3 summarizes the main features and procedures applied in scientific works. Some of these techniques not only detect simple blinks, but they are also capable of classifying voluntary blinking in the form of long blinks and/or winks [4], [49].

Several conditions greatly influence the outcome of these procedures: the subject's distance from the camera and the room's lighting. The article in [51] shows the extent to which they can influence accuracy.

An important characteristic to consider, when evaluating these procedures, is how long it takes them to complete the detection. However, as computer performance, in which the algorithms run, varies from one paper to another, it is very difficult to show a comparative among them. Some authors applied their algorithms using previously recorded or public datasets [16], [77] whereas others used real-time video signals [16], [37].

Many of these investigations were attempting to obtain information about the patient's condition or develop systems facilitating communication between people and computer systems, but very few of them [36] included people with disabilities in their experiments. A wide range of applications can be found by focusing on the control of systems through blinking. Some of these include a hands-free application for mobile devices [51], systems that detect voluntary blinks and interpret them as control commands for the mouse [49] or the keyboard [36]. The latter Computer Interface [36] is available for free download and use.

All this information is summarized in the Table 3. As it shows, the accuracy of some of these systems exceeds 99% [4], [16]. However, this value drops to 95.35% for the test groups that contain people with disabilities [36].

### III. MATERIALS

This section contains a description of the systems developed for IR, EOG, the EEG headset and the software for VOG.

#### A. BLINK DETECTOR BASED ON THE CORNEAL REFLECTION OF INFRARED LIGHT

For eyelid movement measurement, an infrared (IR) emitting diode (model VSMB2020X01) and a phototransistor (VEMT2520X01) were mounted on some 3D glasses (Fig. 1). These IR elements were placed more than 2 cm away from the eye and were approximately aligned with the right area of the right-eye pupil. To do so, the IR elements were mounted on a structure giving them two degree of freedom (DOF) and allowing their placement in an area in front of the right eye. With open eyes, the phototransistor mainly captures the reflected IR radiation coming from the cornea. With closed eyes, most of IR radiation is absorbed by the eyelid skin, reducing the reflected component. Therefore, opening/closing the eyes influences the amount of reflected IR signal and makes the phototransistor current change between high and low values.

**TABLE 3.** Summary of the main features and algorithms for VOG. For the methodology column, step 1 shows how the head/eye is detected, while step 2 describes the procedures for eye blink detection. Some acronyms used in that column: Correlation with templates (CorrT), Counting pixels (CP), Difference between frames (Diff), Eye Aspect Rate (EAR), Finite State Machine (FSM), Histogram Backprojection (HB), Histogram of Oriented Gradient (HOG), Hue Histogram (HH), Hue-Saturation Histogram (HSH), Hidden Markov Models (HMM), Horizontal-Vertical Profiles (HVP), Image Data Set (IDS), Invariant Feature Transform (SIFT), Lucas-Kanade (LK), Median Blur Filter (MBF), Optical Flow (OF), Sum of squared differences (SSD), Support Vector Machine (SVM), Threshold the eye image (TEI), Variance of motion vectors (VMV), Viola-Jones Detector (VJD).

Citation	IDS	#Subjects	Methodology	Accessibility?	Accuracy	Available?	Comment
Ayudhya et al.[4]	No	NA	Step1 VJD, CAMshift Step2) MBF, TEI, CP, FSM	Short blinks Long blinks	99.6%	No	The eyelid's state detecting value
Chat et al.[11]	No	8	Step1) Diff Step2) Erosion, CorrT	Short blinks Long blinks	95.3%	No	Result without sessions involving the testing of the voluntary blink length parameter
Drutarovsky et al.[16]	ZJU Eyeblink8 Talking Face	20 4 1	Step1) VJD Step2) LK, VMV	Short blinks	93.45% 99.5% 99%	No	The method has lower false positive rate compared to other methods
Grauman et al.[24]	No	15	Step1) Diff, Erosion, Geom. Rules Step2) CorrT	Short blinks Long blinks	95.6%	No	Authors also studied eye raising and obtained an accuracy of 93%
Królak et al.[36]	No	49-12	Step1) VJD Step2) CorrT	Short blinks Long blinks	95.35%	Yes	The system was deployed to market as an open-source software for people with disabilities under the name b-Link
Lalonde et al.[37]	No	22	Step1) HVP, SIFT Step2) Diff, OF, CorrT	Short blinks	97%	No	Part of a multi-sensor system to test driver performances
McDuff et al.[46]	No	NA	Step1) VJD, Landmark detector Step2) HOG, SVM	NA	NA	Yes	This software processes the images in order to classify them according to the emotion found using facial recognition
Missimer et al.[49]	No	20	Step1) Erosion, LK Step2) CorrT	Long blinks Winks	96.6%	No	Allows to simulate a mouse
Mohammadi et al.[50]	No	17	Step1) VJD Step2) RGB-> YCbCr Threshold Y histogram	Short blinks	98.91%	No	The advantages are: simplicity, accuracy, fastness, low computational cost and robustness against lighting conditions
Mohammed [51]	No	NA	Step1) VJD Step2) TEI, MBF, CP	Short blinks	98%	No	Results with the best light condition
Morris et al.[56]	No	5	Step1) Diff, Threshold Step2) Variance, LK, OF	Short blinks	90%	No	Accuracy drops to 75% with head movements
Pauly et al.[67]	CEW ZJU	2423 20	HOG, SVM	Short blinks	100% 85.5%	No	This is the best method of 5 tested methods
Sayahzadeh et al.[77]	SBD ZJU Talking Face	59 20 1	Step1) VJD, Diff Step2) Erosion, Dilatation, CorrT and SSD criterion.	Short blinks	98.59% 96.03% 97.99%	No	The innovation of this system is that conditions are not limited and this system increases processing rate
Soukupov [83]	300-VW ZJU, Eyeblink8	50 20, 4	Step1) Landmark detector Step2) EAR several frames, SVM	Short blinks	NA ROC curves	No	Detectors ( <i>Cheltra</i> [3] and <i>Intraface</i> [97])
Yijia et al.[86]	MAHNOB-HCI	12	Step1) EyeAPI [88] Step2) OF, HMM, SVM	Short blinks	90,99 %	No	Models eye blink dynamics Tests several procedures
Polatsek [70]	Talking Face Own IDS	1 8	Step1) VJD Step2) a) HB, HSH, HH b) LK, OF	Short blinks	98.36% (OF) 93.75% (OF)	No	Compares two methods. Results showed that OF is better than HSH or HH



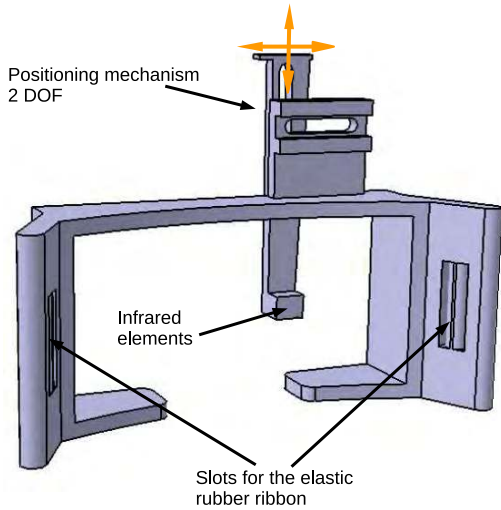


**FIGURE 1.** Virtual reality 3D glasses adapted with a structure that allows the horizontal and vertical placement (2 degrees of freedom - DOF -) of the IR elements in front of the right eye.

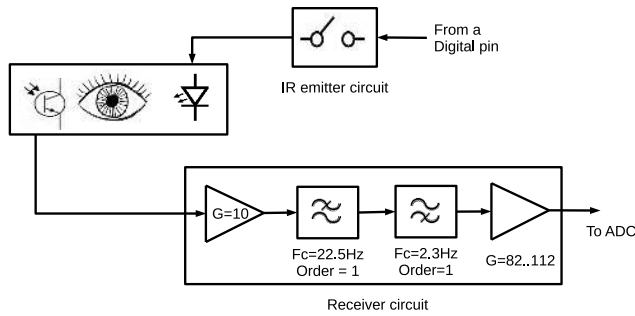


**FIGURE 2.** Building blocks of the IR detector circuit.

The infrared radiation is kept below  $12 \text{ mWcm}^{-2}\text{sr}^{-1}$  which prevents the retina, cornea and lens from being damaged according to European norm EN 62471:2008 [35]. The radiant flux,  $188\mu\text{W}$ , and the irradiance at the eyes,  $0.48 \text{ mW/cm}^2$  are less than the maximum permissible exposure ( $586 \mu\text{W}$ ) and the accessible emission level ( $1.54 \text{ mW/cm}^2$ ) respectively. This means that the system can be classified as class I [9] and the safety of its use for long periods can be guaranteed.

Figure 2 shows the different parts of the circuit, the exact schematic layout is shown in Appendix A, Fig. 19. It has two parts: an emitter and a receiver. The emitter circuit is very simple. It only contains a transistor controlled by a digital input that, when it is high/low, turns the emitter on/off. The receiver circuit is made of different amplifiers and filters.

Current coming from the phototransistor is first converted into voltage and amplified ten times and low-pass filtered at a cut-off frequency of 22.5Hz. It goes through a high-pass one-order filter with a cut-off frequency of 2.3 Hz which filters out low frequency alterations on the reflected IR signal when the position of the eye (or eyelid) changes due to a variation in the eye-gaze. The filtered signal is amplified one more time with a gain which can be adjusted up to roughly 100. The signal

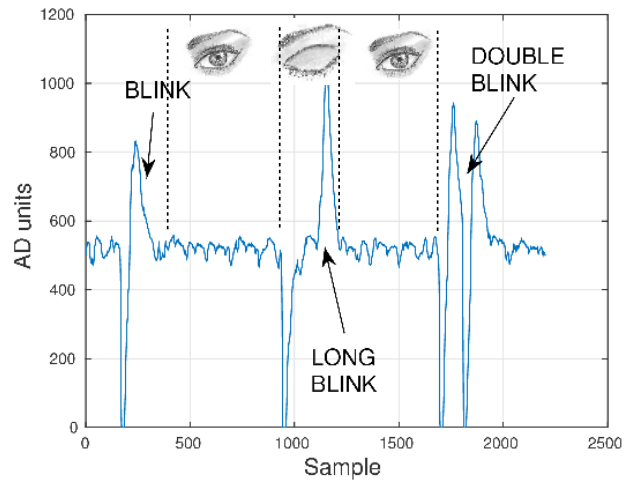


**FIGURE 3.** Output IR signal showing single, long and double blinks.

is finally sampled at a rate of 250Hz using an open-source hardware platform like Arduino.

Figure 3 shows a typical segment of the signal delivered by this device when performing the experiment. A blink contains two waves: a negative high amplitude deflection from the baseline (N wave), followed by a positive one (P wave). Each wave is associated with the action of opening or closing the eyes. In long blinks, the positive and negative waves are further apart than in short blinks.

The algorithm searches for the positive and negative waves, using an adaptive K-means clustering method that classifies samples as belonging to negative or positive waves or baseline. The position of the peaks is then obtained to measure the distance between the N-P waves. A short or long blink is detected if the distance between N-P peaks is more/less than a threshold. The exact algorithm is described in Appendices A and E.

## B. BLINK DETECTORS BASED ON BIOELECTRICAL SIGNALS

In this section we introduce several devices that measure the bioelectrical activity associated with the aperture and closure of the eyes.

### 1) BLINK DETECTOR BASED ON EOG

Figure 21, in Appendix B, shows the schematic layout of the developed circuit, which is based on one published in [71] but incorporating a band-pass filter with a frequency range between 0.6-15Hz in the final stage. It uses three electrodes, type Ambu 71508-K/C/12, that are positioned as shown in Figure 4, with a reference electrode at the temple and the two others placed above/below the eye.

The EOG circuit amplifies the electrical ocular activity that, due to the electrode placement, is influenced more by vertical eye movements and blinks. The analog signal is sampled at a rate of 250Hz using an open-source hardware platform like Arduino.

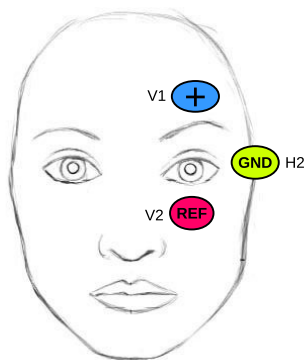


FIGURE 4. Electrodes placement for EEG.

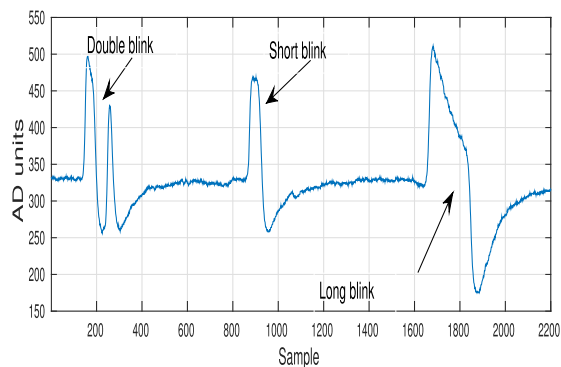


FIGURE 5. Output EOG signal showing double, short and long blinks.

Fig. 5 shows a typical EOG signal containing short and long blinks. They are characterized by short or long positive pulses. However, the high-pass filter implemented in the circuit tends to remove the DC component of the pulses, which makes them have positive and negative deflection from the baseline. This is especially significant for long-blinks as can be seen in Figure 5.

The algorithm is described in Appendices B and E, and is basically the same as that shown in the section above for IR signals. The difference is that, initially, a Savitzky-Golay filter [78] is applied to obtain the derivative of the signal, which contains positive and negative waves like the IR signal in Figure 3.

## 2) BLINK DETECTOR BASED ON A COMMERCIAL EEG HEADSET

EEG headsets under \$1000 are available for consumers. The cheapest one is NM which costs approximately \$100 and has been developed as a non-invasive tool with a dry electrode located on the left side of the frontal area corresponding to FP1 position according the 10-20 system. It provides information through a Bluetooth connection that can be classified in three levels of processing. From the lowest to highest levels, they are: 1) raw EEG signal sampled at 512Hz, 2) power bands ( $\delta$ ,  $\theta$ ,  $\alpha$ ,  $\beta$  and  $\gamma$ ), and 3) the eSense Brainwave patterns of attention and meditation. Power bands and eSense signals help reduce the preprocessing of the raw

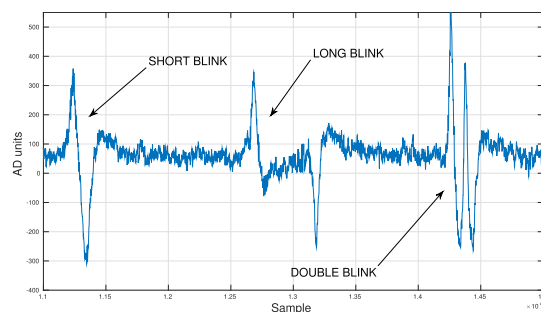


FIGURE 6. A typical raw EEG signal delivered by NM containing several types of blinks.

signals in external devices and allow digital systems with low computation resources to be used, also minimizing the costs and time of the analysis. As the electrode position is near the left eye, it also picks up ocular movements and blinks contaminating the EEG signal. In EEG processing, artifacts must be removed from the epochs or alternatively the epochs containing artifacts must be tagged in order to exclude them from the analysis. The manufacturer also provides an algorithm for signaling the existence of short blinks in the EEG signal if required. This helps identify contaminated epochs or might also be used as a control signal for accessing a computer.

Figure 6 shows a typical EEG signal from NM containing blinks and one long blink. A blink is characterized by three waves: an initial high amplitude positive deflection from the baseline, followed by a high negative one and a final small positive wave. For long blinks the high amplitude deflections are more separated and small inverted waves follow such deflections. The NM proprietary algorithm can signal short blinks but is unable to distinguish between long and short blinks.

## C. BLINK DETECTOR BASED ON IMAGE PROCESSING

The last alternative to explore is the blink detector based on image processing. As shown in Table 3, there has been a lot of work here, but only a small number of authors have allowed access to their code under some type of open source license. When authors do provide this access, they are helping other researchers to advance from a verified starting point, speeding up new lines of research.

Table 3 shows the existence of open-source solutions with the code available for the community [46] and [36]. The former is not specific for AAC and for this reason there is no information about the blinking detection accuracy, whereas the latter is specific for AAC with an accuracy over 95%. However, we did not use it due to a lack of performance found during the initial trials. In addition, we were not able to find the whole code of the application in order to adapt it to our needs.

The other alternative (Table 3) is a real-time facial expression recognition toolkit developed by Affectiva<sup>1</sup> [46].

<sup>1</sup> Available on March, 2018: <https://developer.affectiva.com/>

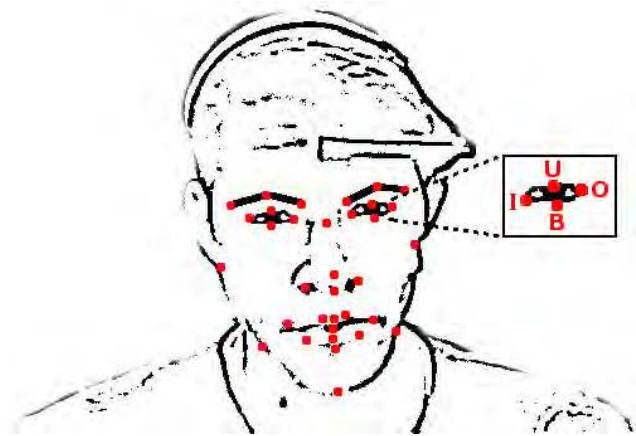


**FIGURE 7.** Face landmarks obtained with AFFDEX SDK. For each eye four landmarks are returned: *U* and *B* indicate upper and bottom centers of eyelids, and *O* and *I* mean outer and inner eye points.

This is called AFFDEX SDK (AF-SDK), which runs in the most important operating systems (Android, iOS, Linux, and Windows) and supports several image formats: static photos, recorded video or on-line video-camera. The developers recommend an RGB camera with a resolution greater than 320x240 pixels, that the subject's face covers at least 30x30 pixels, and a sampling rate greater than 10 frames per second. Practically, any inexpensive webcam fulfills such requirements, like the webcam model Logitech V-U0003 we used in the experiments.

AF-SDK is based on a subset of action units (AUs) defined in Facial Action Coding System (FACS) to evaluate facial expressions [17]. We used the first stage in the AF-SDK processing pipeline for locating face landmarks. For blink detection we calculated the EAR [83] as the average of the ratios between the minor and major axis of the two ocular ellipses. Eq. 1 shows the expression used for one eye, where *EL* is eye landmark, *x* means left or right eye and superscripts identify the ocular landmarks shown in Figure 7.

$$EAR_x = \frac{|EL_x^U - EL_x^B|}{|EL_x^O - EL_x^I|} \quad (1)$$

To detect short, long blinks we set a classifier based on an adaptive K-means method with two centroids. One of them identifies the baseline and the other the blink itself. The length of grouped blink samples discriminates long blinks from short ones. A more detailed explanation can be found in Appendices D and E.

#### IV. PARTICIPANTS

We split participants in the experiment into two groups with slightly different research goals. The first group was formed by people without disabilities and they performed the experiment before the other group. They tested the technologies several times to obtain the performances and user preferences. Participants were not given any feedback about whether the

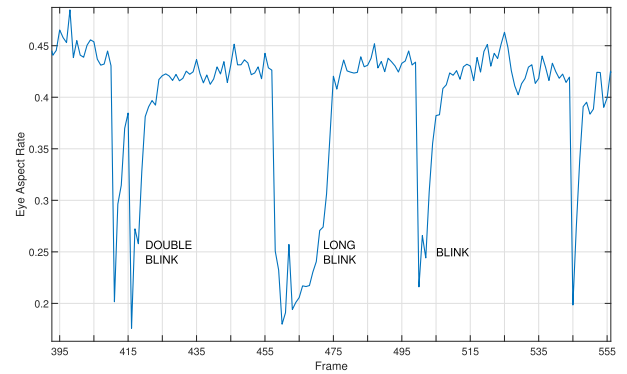


**FIGURE 8.** EAR signal obtained with Eq. 1.

system was recognizing voluntary blinking. This was done for two reasons. Firstly, to make the blinking as natural as possible and to prevent the subjects from adapting their blinking to the technology. Secondly, to find out which system and blinking method were preferred according to aspects such as comfort, fatigue, ability, etc. without any bias in favor of a specific technology due to its accuracy.

The other group included people with disabilities and the main goal was to gain knowledge about which system had the potential to be included in their daily activities when interfacing a computer or a communication board. Here, participants received feedback on how the system interacted with them.

All participants agreed to take part in the experiment and, in the case of people with disabilities, their families were informed and signed the consent form. The Ethics committee of the *Regional Government of Andalusia* approved the experiment.

#### A. PARTICIPANTS IN EXP1

Seventeen people with ages ranging between 24 and 51 years, 6 females and 11 males, took part in experiment Exp1. Most of them were undergraduate students recruited from School of Computer Engineering at the University of Seville.

#### B. PARTICIPANTS IN EXP2

People with disabilities were recruited from different associations that take care of them near the city of Seville (Spain).

##### 1) AMMIOTROPHIC LATERAL SCLEROSIS

Four people with ages ranging between 26 and 66 years (Table 4) were recruited from the association *ELA Andalucía*, which has around 160 members and gives support to up to 400 people in Andalus. It is a policy of the association not to use AAC systems, based on residual movements, with people in a non-advanced stage of the disease. Moreover we were told that in general the use of AAC alternatives is rejected by this collective. For these reasons we were given a reduced list of potential candidates.

One of the participants has the spinal form of the disease (limb onset) [95], another has the Duchenne muscular

**TABLE 4.** Description of participants with ALS.

Subject	ALS type	Diagnosis time (years)	Anarthria
MRM	Bulbar	3	yes
MLI	Medular	4	yes
NTN	Medular	9	no
AFL	Duchenne	26	no

**TABLE 5.** Description of participants with cerebral palsy according to GMFCS and CFCS.

Subject	GMFCS	CFCS
RBB	V	II
MNR	V	III
PLS	V	III

dystrophy [18] and the rest the bulbar onset variant of ALS. All of them need some support for breathing and feeding. AFL has dysarthria but he can get his thoughts across perfectly. He uses a high sensitivity mouse pad, on a bluetooth keyboard, to access a computer by performing very low-amplitude movements with his right-hand fingers and also uses a voice-to-text application for writing. MRM can move her hands roughly but is able to write messages in a mobile phone or tablet. MLI uses a head-controlled laser to point out a character printed on a piece of sheet placed on the wall. She also has an eye tracker but scarcely uses it because it is complex to set up and her husband, who takes care of her, is not capable of doing this. There is a clinical suspicion that she also suffers from frontotemporal dementia (FTD) which sometimes goes with ALS. NTN can use a powered wheelchair through a joystick controlled by his chin. The cannulae in his throat prevents him from speaking normally but it is not difficult to understand what he wants to say just by reading his lips. At the moment he does not use any kind of AAC system or input device for accessing a computer.

## 2) CEREBRAL PALSY

We recruited 3 people with cerebral palsy from a school called *Colegio de Educación Especial Directora Mercedes Sanroma* dedicated to work with motor disability students in Seville. All participants with CP had good intellectual, visual and hearing capabilities but very poor motor skills, including the inability to speak. Table 5 summarizes their description according to Gross Motor Function Classification System (GMFCS) and the Communication Function Classification System (CFCS).

The Gross Motor Function Classification System [62] is a 5-level clinical classification system that describes the gross motor function of people with cerebral palsy on the basis of self-initiated movement abilities. Particular emphasis in creating and maintaining this scale rests on evaluating sitting, walking, and wheeled mobility. Distinctions between levels are based on functional abilities; the need for walkers, crutches, wheelchairs, or walking sticks. At level I, balance and coordination are limited, although children perform gross

motor skills such as running and jumping. At level V, children are limited in their ability to maintain antigravity head and trunk postures, control leg and arm movements.

The Communication Function Classification System [28] is a tool used to classify the everyday communication of an individual with cerebral palsy into one of five levels according to effectiveness of communication. For example, at Level I, a person independently and effectively alternates between being a sender and receiver of information with most people in most environments. However at Level V, a person is seldom able to communicate effectively even with familiar people.

RBB is a 15-year-old girl with dystonia [75]. She can execute coarse movements with left-side body limbs and has bad control of her head position. She can voluntarily close and open her eyes but in an asymmetric way, showing more control over her right eye, which is closed before the left one and for longer. When performing this action, other facial and head movements are involuntarily executed.

MNR is a 17-year-old girl who has muscle spasticity [75], no postural head control and difficulty in reaching a switch to access a computer. She has voluntary control of her eye movements, although closing them implies uncontrolled head movements. She followed the strategy of leaning her head against the headrest of the wheelchair to reduce the amount and severity of her involuntary movements.

PLS is a 20-year-old woman with dystonia [75] who cannot control any part of her body continuously, excluding some slow head movement and upper limbs and showing the asymmetric tonic neck reflex frequently. She usually communicates through eyes answering simple yes/no questions by just looking upwards to say yes.

## V. METHODS

The experiment was split in two parts. People without/with disabilities participated in the first/second part, which, in general, was aimed at gauging the performance of the proposed systems, their usability and to gain knowledge about the best method of voluntary blink detection. Differences between both parts are given below.

### A. EXPERIMENT EXPI

Participants without disabilities were asked to perform one of the three following actions: a single short blink, a sequence of two short blinks or a long blink. A Matlab GUI application was built to show participants the action to perform while they were sitting on a chair at a distance between 50-80cm away from a 22" screen. The room was kept at a comfortable temperature ( $T = 20^{\circ}\text{C}$ ) and with artificial lighting at 700 lux, measured with an application called *Photometer* running in a Samsung Galaxy s6 mobile phone.

Subjects looked at a cross as a reference point on the screen. A character then appeared for 1s in the position of the cross indicating the action to be performed. The time between stimuli,  $T_{isi}$ , was set equal to 3s to minimize the incidence in natural blinking (which has a frequency roughly equal

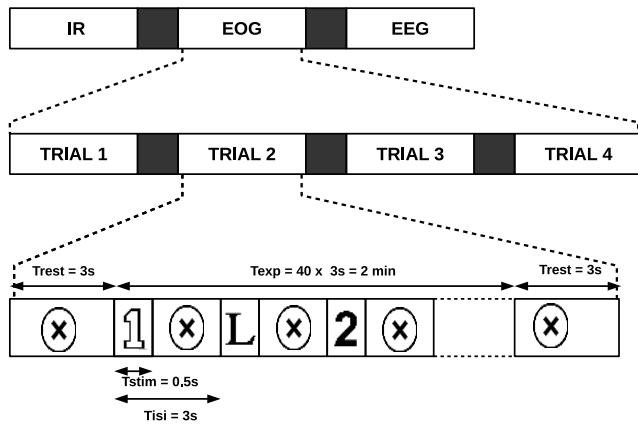


**FIGURE 9.** The temporal sequence in Exp1. Subjects were randomly asked to perform three actions: Short (1), long (L) and double (2) blink in each trial. There were four trials for each technology and as all of them were recorded by a webcam, it was not necessary to add more trials to test VOG.

to 17 blinks/min or 3.53 s/blink in normal people at resting [6]). Each trial involved performing 40 actions which, when added to an initial and final 3s resting period, meant that the trial lasted 126s. Figure 9 depicts the temporal sequence in the experiment. Actions were randomly distributed through the trial and an experiment consisted of four trials. Participants repeated the experiment with each device (IR, EOG and EEG) over several days, so overall they each performed 12 trials.

In all experiments and technologies both raw signal and algorithm output were stored. The former could be analyzed further to improve the detection algorithm if needed. A webcam recorded each experiment with the three-fold aim of validating the captured data, guaranteeing the veracity of the experiment and obtaining the performances for VOG.

Signals, video and the GUI were all synchronized and segmented using labstreaminglayer [34], [48]. Two experts validated all segments to guarantee that they did not contain extra blinks or incorrect actions.

Finally, participants were asked to say which method of accessing they would choose if they had to, and which action (double or long blink) would be better for them.

**B. EXPERIMENT EXP2**

The second experiment was performed by people with disabilities. The main goal was to find out which technology (VOG, IR-OG, EOG, EEG) and interaction method (double or long blink) was preferred by users.

Firstly, participants were told that the experiment was about the assessment of a set of technologies allowing computer access through blinking. We made it clear that we did not want them to include the communication board as part of the assessment since it was only used to collect data for the analysis. To illustrate the potential use of blinking as AAC, we played a promotional video showing the ACAT software and its capabilities as a communication system, to manage desktop applications or for surfing

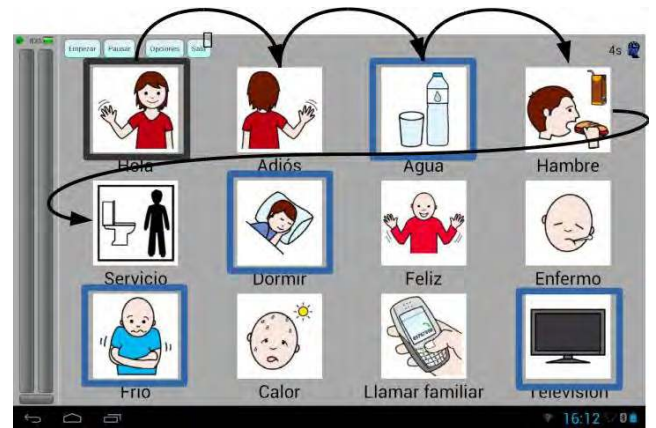


**FIGURE 10.** Communication board containing the target ideograms in blue and illustrating the serial scanning process.

on the web. The video can be downloaded from the following url: <https://01.org/acat/documentation/acat-features-overview-new>

Secondly, we told them about the four technologies and how to interact with them using long or double blinks. They then decided which of them they wanted to use and the method of voluntary blinking. Before starting the experiment, they practiced several times to get used to the timing of long and double blinks. Participants were shown a communicator board on the computer screen, with 12 frames containing ideograms (see Figure 10) or text, depending on their skills. Four of these ideograms were selected as targets and appeared marked in blue, although if they wanted to choose other targets they were able to do it. The communicator implemented the serial scanning of its frames with a configurable dwell time ( $T_{scan}$ ). As soon as the scanning reached the target, the participant had to make a voluntary blink. As a feedback, the system played a sound related to the information contained in the frame when the voluntary blinking was detected. When the scanning reached the final frame, a new panel with different content was again shown on screen. Overall 4 different screen panels were shown and subjects performed at least two sessions on different days.

In the last session, the participants were asked about their preferred technology and method. Without taking into account the time taken to test and prepare each technology, the experiment took between 20-25 min for participants to complete.

**VI. RESULTS**

We analyzed the feasibility of the different methodologies with people without/with disabilities. Data obtained from Exp1 served mainly to configure and adjust the devices, get to know their performances, users' preferences and compare methods of voluntary blinking (double blink vs. long blink). The people with disabilities were then given the adjusted devices in a new experiment, Exp2, in which the collected data were analyzed to obtain the performances and subjects' preferences as well, but, in this case, participants

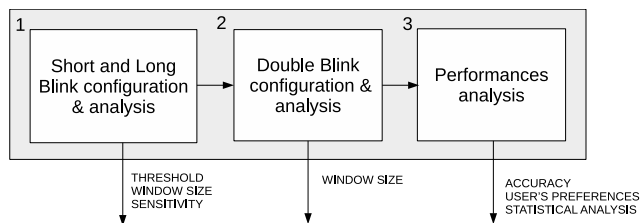


FIGURE 11. Flowchart describing the steps followed in the analysis of data in Exp1.

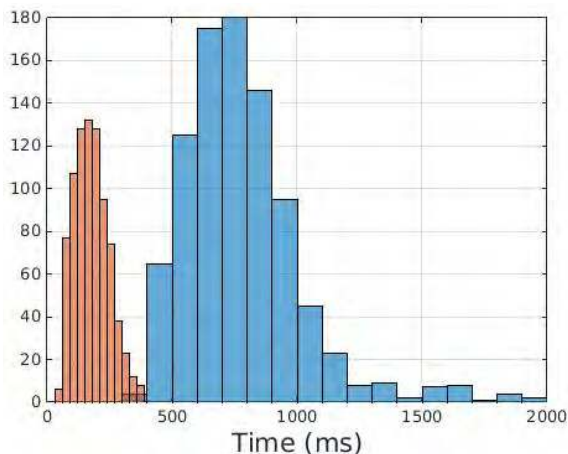


FIGURE 12. Histogram of short- and long-blink duration.

had the feedback of how the different systems worked. Experimental data can be downloaded from the following link: [https://www.researchgate.net/publication/331320020\\_Experiments\\_blinking](https://www.researchgate.net/publication/331320020_Experiments_blinking).

A. EXPERIMENT EXP1

Figure 11 depicts the flow chart describing the procedure to adjust the technologies and assess the performances. In the first step, we focused on obtaining the duration for short and long blinks, on determining the necessary length of the data (window size) allowing their detection, and on setting the appropriate threshold to accurately discriminate them. In the second step, the double blink was studied and we analyzed the window size that the algorithm needs to wait for the second blink to come. Finally, we studied the accuracy of the four technologies and users’ preferences and performed a statistical analysis on the benefits of using one or another method or technology.

1) SHORT AND LONG BLINK CONFIGURATION PARAMETERS

The way in which participants performed blinks did not depend on the technology used. However, the estimation of the blink duration may reveal differences depending on the technology or the procedure applied. For example, in IR-OG every blink is characterized by a negative deflection of the signal followed by a positive one (Figure 3) and the difference between them allows the algorithm to distinguish a short from a long blink, as the histogram in Figure 12 shows.

To explain in more detail how the blink duration was obtained, we need to describe the operation of the IR-OG algorithm. Figure 20 includes the results at different stages of the algorithm for a double blink. Firstly, it classifies samples into three classes: P, none, N, according to the distance to three centroids. Then, all the sample belonging to the same class are gathered and labeled as P or N waves. All blinks contain an N and a P wave, and the distance between them defines the type of blink (short or long). The histogram in Figure 12 shows the distances between the first sample of the N wave and the last one belonging to the next P wave. Obviously, the estimated blink duration is slightly less than the real action, since some associated samples at the start/end of the movement, which are very close to the baseline, are not included in the N and P waves. As one can see in the Appendices, the algorithm for EOG is basically the same as for IR-OG and the blink duration estimation follows the same procedure. However, in VOG, the algorithm only uses two centroids, classifying each input sample in two classes (blink, baseline). Here, the duration of the blink depends on the number of samples that belong to the blink class.

On average, a short blink lasts 176.3ms whereas a long blink lasts 776ms. A threshold to differentiate between those types of blinks must be set somewhere in the middle, following the criteria to minimize the number of false positives. For IR-OG such a threshold was set at 392 ms (98 samples for a  $F_s = 250\text{Hz}$ ), 95 samples for EOG ( $F_s = 250\text{ Hz}$ ) and 6 samples (frames at  $F_s = 15\text{ fps}$ ) for VOG. One has to remember that the EEG headset has a proprietary algorithm for detecting short blinks and is not able to differentiate between short and long blinks.

Another aspect concerns the upper limit of the temporal window used to search for a P wave. In other words, how long it is necessary to wait for the P wave once the N wave has been detected. To illustrate of the distance between N-P waves, Figure 12 shows that some long blinks lasted around 2s. We followed the criteria of establishing a window size that included more than the 99% of all long blinks. According to this criteria, the empirical value for such a limit was of 2s for IR-OG, EOG and VOG. This meant that after the detection of an N wave, the algorithm had to wait for a P wave to come for 2s. If such a wave was not received, the algorithm started looking for a new N wave.

After setting the threshold and the upper limit, data collected and annotated by two experts were compared with the offline algorithm outputs. Table 6 shows the sensitivity in recognizing the short and long blinks for each participant. Sensitivity measures the percentage of correctly predicted outcomes compared to the number of inputs in each class.

For the proposed IR-OG technology, the algorithm was able to detect 98.6% and 98.2% of short and long blinks respectively. Only for subject 9 was the percentage less than for the rest of the participants. This was because the signal showed several peaks and the algorithm found them difficult to classify as long blinks.

**TABLE 6.** Sensitivities or proportion of true single and long blinks per subject in Exp1 that were correctly identified using the four proposed technologies.

Subject	IR		EOG		EEG	VOG	
	S-blinks (%)	L-blinks (%)	S-blinks (%)	L-blinks (%)	S-blinks (%)	S-blinks (%)	L-blinks (%)
1	100	100	100	0	100	100	96.9
2	100	100	100	80.9	82.7	88.5	100
3	100	98.8	97.9	54.6	97.7	NA	NA
4	100	100	100	98.2	100	100	92.7
5	100	92.7	76.9	53.1	93.3	100	100
6	92.5	100	97.8	16.2	83.8	95.8	95.9
7	100	94.3	100	94.1	100	100	96.2
8	100	100	100	92.6	100	93.3	100
9	88.5	75	100	96.5	97.4	95.8	93.1
10	100	100	100	90.9	98.1	100	100
11	100	100	94.7	92.9	30.6	71.4	100
12	100	100	96.9	86.2	89.8	91.4	96.3
13	96.7	100	100	28	70.2	98.2	94.6
14	100	93.8	100	95	100	100	100
15	100	100	100	85.3	92.5	98	100
16	94.1	98.4	100	100	96.1	92.2	100
17	100	100	92.9	64.3	94.6	96.2	100
<b>Total</b>	<b>98.6</b>	<b>98.2</b>	<b>97.4</b>	<b>76.5</b>	<b>89.8</b>	<b>95.4</b>	<b>98.6</b>

The detection of long blinks in EOG, by adapting the algorithm used in IR-OG, did not obtain such good results as IR-OG. Indeed, the sensitivity percentage was 97.4% and 76.5% for short and long blinks respectively.

The total sensitivity in detecting short blinks when using the proposed EEG technology was 89.8%. Finally, for VOG, the sensitivity in detecting short and long blinks was 95.4% and 98.6% respectively.

2) DOUBLE BLINK CONFIGURATION

At a higher level of processing, double blinks need two single blinks to happen within a short period of time. Figure 13 shows the double-blink duration histogram. On average, a double blink takes 463 ms, which is more than twice the duration of a single blink. To avoid false negatives, and increase detection accuracy, a 1.2s-long temporal window was set for all technologies. Therefore, when a single blink is detected a timer starts. If a second single blink is received before the timer expires, then a double blink will be signaled.

3) PERFORMANCES, USERS' PREFERENCES AND STATISTICAL ANALYSIS

Once the algorithm had been properly configured, the confusion matrixes for each methodology were obtained. Tables 7, 8, 9 and 10 show the results for each methodology. For IR-OG, a classifier that considers the three types of blinking obtained an accuracy of 98.6%. However, the technology could only work detecting one type of voluntary blinking. In such a case, for a system detecting only double blinks the accuracy was 99.3% while for long blinks, it was 97.9%. Overall, only 34 out of 2477 short, double or long blinks were misclassified.

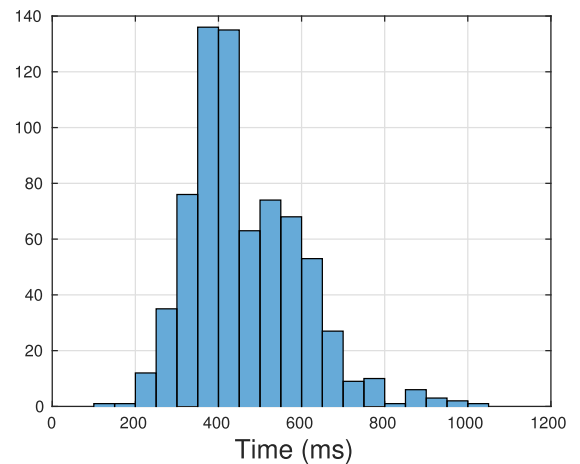


**FIGURE 13.** Histogram of the double-blink duration.

**TABLE 7.** Confusion matrix for the IR-OG detector when discriminating three types of input events.

	Predicted			
	SB	LB	DB	None
SB	828	9	0	3
LB	14	900	0	3
DB	5	0	715	0

For EOG, a classifier considering the three classes had an accuracy of 89.9%. For double blinks the accuracy was 97.2% whereas for long blinks it was 76.6%. Overall, 182 out of 1799 short, double or long-blinks were misclassified.

For EEG the global accuracy was 88%, but considering the short blinks and double blinks separately the accuracy was 83.3% and 85.9% respectively. Overall, 170 out of 1419 short or double blinks were misclassified.

For VOG the detection accuracy for three types of events was 95.7%, but for long or double blinks alone the

**TABLE 8.** Confusion matrix for the EOG detector when discriminating three types of possible input events.

	Predicted			
	SB	LB	DB	None
SB	644	1	0	16
LB	101	491	0	50
DB	6	0	482	8

**TABLE 9.** Confusion matrix for the EEG detector when discriminating two possible input events.

	Predicted		
	SB	DB	None
SB	702	0	80
DB	61	546	29

**TABLE 10.** Confusion matrix for the VOG detector when discriminating three types of possible input events.

	Predicted			
	SB	LB	DB	None
SB	753	20	0	16
LB	12	847	0	0
DB	21	28	589	1

**TABLE 11.** Maximum accuracies in detecting voluntary blinking for the four tested technologies. <sup>1</sup>Long blink input is not possible.

Techn.	Accuracy (%) / $F_1$ score	Input type
IR-OG	99.3 / 0.997	Double blink
EOG	97.2 / 0.986	Double blink
EEG	85.9 / 0.924	Double blink <sup>1</sup>
VOG	93.4 / 0.966	Long blink

accuracies were 93.4% and 92.2% respectively. Overall, 105 out of 2318 were classified incorrectly.

Table 11 summarizes the accuracies and type of voluntary input with the best performances in each technology. Table also contains the  $F_1$  [87] score, which is the harmonic mean between the precision (the percentage of correct outcomes) and sensitivity of the classifier, reaching its best value at 1 and the worst at 0. In general, it seems that the usage of double blinks obtained the highest accuracy in almost all technologies, excluding VOG. However, according to the Kruskal-Wallis (KW) test, those differences were not statistically significant in IR-OG and VOG ( $p$ -value = 0.17 and 0.59 respectively). Only EOG operated through double blinks outperformed in accuracy the same technology with long blinks ( $p < 0.001$ , KW test). It is also important to highlight the dependence of accuracy on the input method ( $p < 0.001$ , KW test), with IR-OG being the technology with the highest value, followed by EOG and VOG.

Figure 14 shows the survey results. Participants mostly preferred VOG to other technologies and when they were asked about the best wearable there was a tie between IR-OG and EOG. Regarding the type of voluntary blinking, there was a slight bias in favor of long blinks.

A final aspect we were interested in, was related whether there was a significant difference between the time taken to

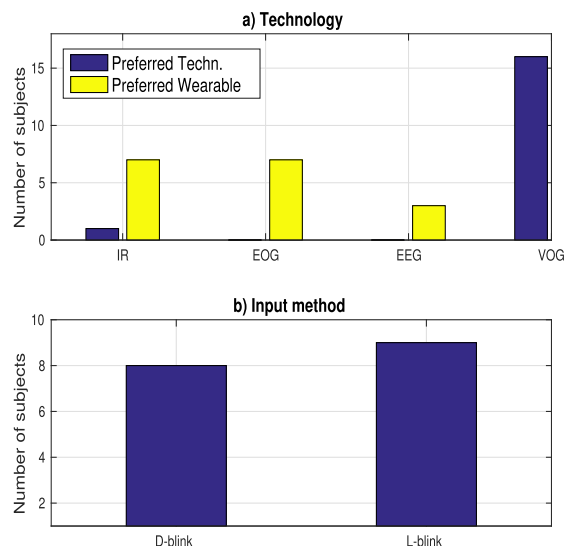


**FIGURE 14.** Participants' preferences in Exp1 according to a) technology and wearable technology, and b) input method (double or long blink).

execute a double blink compared to a long blink. Figure 15 shows the durations of long and short blinks for all subjects. It shows that long blinks took longer than double blinks for all subjects excluding participant #4. For them all, there was a statistically significant difference between those times, with a  $p$ -value less than 0.001 according to the Mann-Whitney-Wilcoxon (MWW) test. Subject #4 also obtained a significant  $p$  value of 0.003. These results suggest that performing double blinks is more efficient for speeding up the interaction with computers and in general, as the fastest method for reacting to a stimulus. However, this was not the preferred method for most participants (Figure 14).

**B. EXPERIMENT EXP2**

As explained in section V-B, participants were shown a communication program based on the serial scanning of its ideograms (or text boxes). A webcam recorded the user's face when interacting with the software and every video frame was synchronized with the scanning process. Hence, experimenters were able to analyze and compare segments of the raw signal, and the classification results, to the video frames to verify correspondence with the performed eye gesture. Each segment of analyzed data coincides with one scanning period. In contrast to Exp1, here the subjects' actions that caused false positives were not filtered out. We wanted to identify and describe the reasons that caused those false positives and bring the developed technologies to a more practical scenario.

From this analysis, the confusion matrixes and the accuracies were obtained. Table 12 summarizes these results, including the personal preferences. In general, wearable technologies were not appealing for the members of this group and most selected the VOG and long blinks as the favorite method of interaction. The ALS subgroup obtained good results for almost all technologies and input methods and



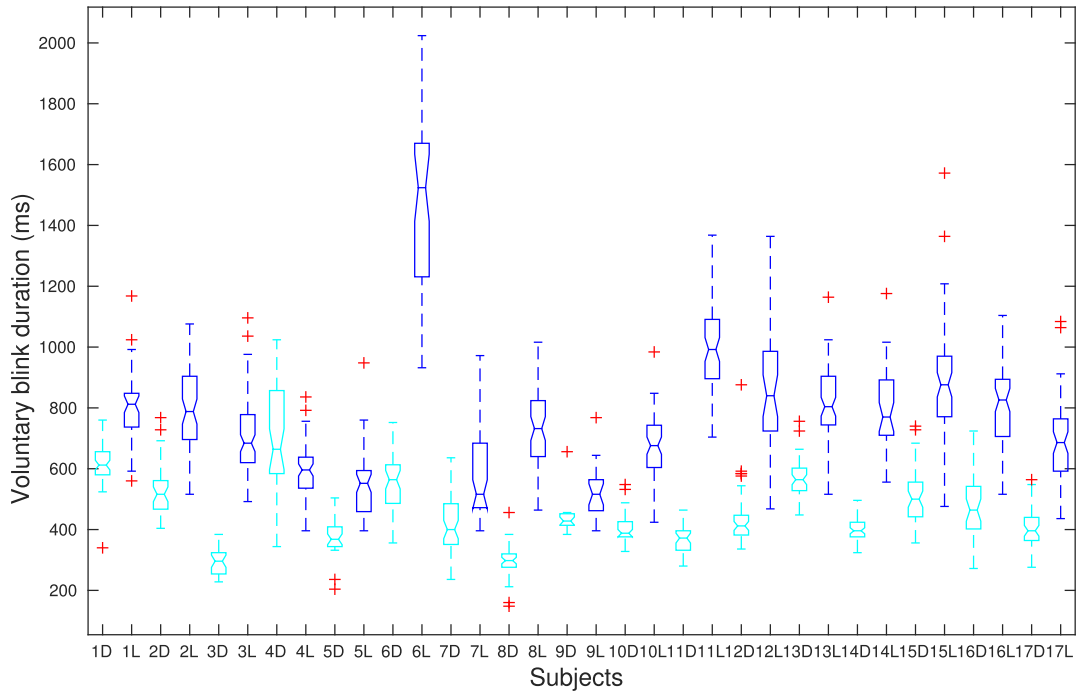


**FIGURE 15.** Boxplot comparing the duration in performing a double and a long blink for each subject in Exp1. In general, double-blink durations (in cyan) are shorter than long blinks (in blue).

**TABLE 12.** Accuracies and  $F_1$  score obtained by people with disabilities in Exp2. Personal preferences have also been included.

			Accuracy (%) / $F_1$ score				Preferences
	Name	Method	IROG	EOG	VOG	EEG	
ALS	MRM	Long	100 / 1.00	75.7 / 0.86	84.2 / 0.91	–	EOG, VOG
	MLI	Long	–	90 / 0.95	81 / 0.90	–	VOG
	NTN	Long	100 / 1.00	64.8 / 0.79	94.1 / 0.97	–	VOG
		Double	95.5 / 0.96	100 / 1.00	80.8 / 0.89	–	Long
	AFL	Long	100 / 1.00	93.9 / 0.97	98 / 0.99	–	EOG
Double		97.2 / 0.99	96.3 / 0.98	83.8 / 0.91	NA	Long	
CP	RBB	Long	62.9 / 0.77	28.9 / 0.45	76.5 / 0.87	–	VOG
		Double	–	100 / 1.00	75 / 0.74	–	Double
	MNR	Long	56.4 / 0.72	37.5 / 0.55	61.5 / 0.76	–	VOG
		Double	–	95.1 / 0.98	80.7 / 0.95	–	Double
	PLS	Long	–	90.5	89.4	–	VOG

there were non-significant differences with the accuracies obtained for people in Exp1 ( $p > 0.05$ , MWW test). Only two people from the CP subgroup preferred double blinks to long ones since the participants showed a high amount of involuntary head movements that, in many cases, mimicked the long-blink signal, as we will explain below.

1) ALS SUBGROUP

NTN tested all the technologies and input methods excluding EEG, because the headrest meant that the headset could not be placed comfortably. He preferred VOG and the use of long blinks to double blinks, although, as can be seen in Table 12, NTN obtained better results with the other technologies. The lowest accuracy was achieved with EOG when using long blinks, because about 28.8% of those signals showed a pattern (pattern #3 in Figure 17) that differed slightly from

the expected one (pattern #1 in the same figure). Another 7.7% of long blinks were false due to other facial gestures, such as raising the eyebrow, that mimicked the long-blink signal. In contrast, there was a low percentage of false single blinks, 2.1% caused when the subject changed quickly the eye gaze to another location. When testing the EOG with double blinks, NTN had no problem performing the second short blink within the preset time interval (accuracy of 100%).

Using IR-OG, NTN obtained very good results with both long and short blinks. All long blinks were correctly identified but the accuracy worsened for double blinks because sometimes NTN did not completely open his eyes between blinks. Figures 3 and 20 show a normal double-blink IR-OG signal while Figure 16 shows the signal when the action was not performed properly. With IR-OG only 1.23% of all single blinks were not correctly identified.

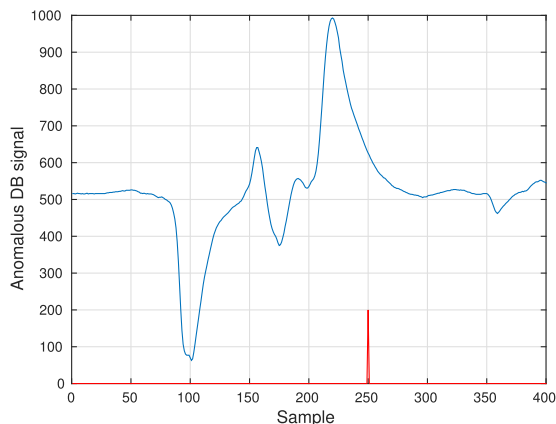


**FIGURE 16.** Anomalous IR signal for a double blink due to the fact that the subject did not completely open the eyelid before the realization of the second blink. The detection result, in red, shows that the gesture was classified as a long blink.

NTN’s favorite method and technology (VOG with long blinks) ranks fourth. Most errors in VOG come from a noisy EAR signal that, compared to other technologies, produces many false single blinks (10.5%) and affects the double-blink detection as well (19.2%). With respect to long blinks, there were two main causes for false positives: a) the action of laughing, which makes the cheek rise up, reducing the eye aspect ratio (EAR) and generating a signal similar to a long blink; b) two double blinks performed very quickly, which fuse the signals together as a long blink.

MRM refused to use the EEG technology because she did not want to ‘look like a robot’ and preferred long blinks as method of interaction. She obtained the best results with the IROG (100% in accuracy) and the worst with EOG (75.2%). Like NTN, most EOG errors (20%) came from a raw signal that follows the pattern #3 shown in Figure 17 which made the classifier identify it as a short blink. As a result of raising an eyebrow or looking at the experimenter temporally, 6.7% of detected long blinks were false positives. When using VOG, the signal was missing for 11% of the experiment’s duration. When this happens, the centroids stop updating until the signal is recovered, and then the value of the EAR may not match the previous signal level, showing a transient step that may be interpreted as a single or long blink. This was an important source of false single blinks (50%) and long blinks (11.1%) which contributed to worsening global accuracy. Additionally, 5.9% of noisy long blinks were classified as double blinks.

MLI was not capable of performing a sequence of two short blinks. The time it took her to voluntarily close and open her eyes was considerably longer than for other people, so, with the current configuration of the system, the use of this input method was not feasible. She refused to test the IR-OG montage and the EEG headset was ruled out by the experimenter for the reasons described above. She preferred VOG to other solutions even though the accuracy was higher with EOG. The VOG signal was missing in 7.6% of the

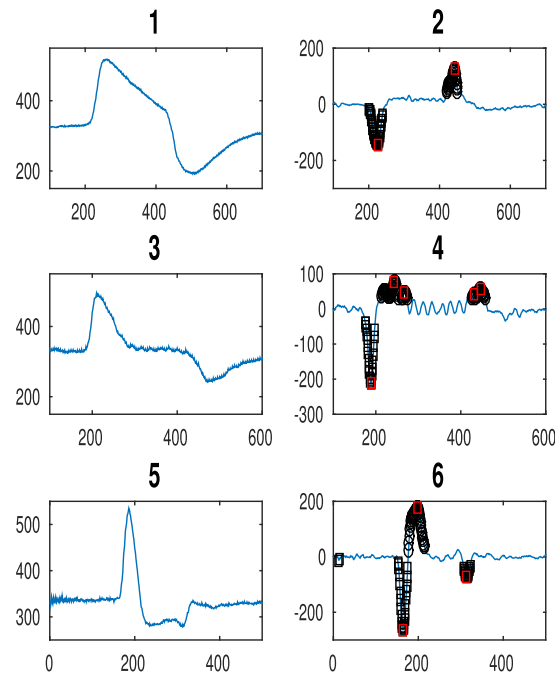


**FIGURE 17.** Several EOG signals patterns for long blinks. 1) A typical long blink signal and 2) its derivative. Samples associated with N and P waves are also marked. 3) An atypical long blink signal whose derivative 4) makes the classifier to predict it as short blink. 5) Subject’s long blink signal that is identified as short 6).

experiment’s duration and the main source of false positives was caused by laughing, which made her cheek rise and slightly close her eyes, generating a signal similar to a long blink. Furthermore, 7.4% of long blinks were confused as doubles due to the noise contained in the signal. With respect to EOG, 5% of long blinks were classified as single blinks, with the same pattern as shown in Figure 17, and another 5% was not recognized for lasting too long.

AFL also chose long blinks as input method based on the belief that the other method might make more false selections. Initially he performed the double blink very quickly. In fact, he had to make more than two or three blinks to stop the system to not confusing them with a noisy single blink. After brief training, he performed the double blink correctly. In general, accuracy was better when using long blinks for IR-OG and VOG and better in EOG with double blinks, although there were no significant differences between them ( $p = 0.4$ , MWW test). AFL tested all the systems and methods of access. For the EEG headset we were unable to obtain any quantitative result because over the two sessions we carried out, we could not get the system to work properly. The blink information was not detected by the proprietary algorithm in most cases, due perhaps to a small blink signal or a poor contact between the sensor and the forehead. Moreover, sometimes the device sent false bursts of blinks when the input EEG raw signal was completely free of them. AFL preferred the EOG even though this method did not outperform the others. In VOG 4.2% of single blinks detected were false: 55.6% of them were caused by fast double

blinks; 33% were when the EAR signal was recovered and the rest were due to long blinks that did not last the required time. The missing long blinks in VOG constituted 2.1% of blinks, similar to the percentage of false long blinks (2%) caused by double blinks that were performed too quickly.

In IR-OG, AFL obtained a percentage of 2% and 0% of missing single and long blinks respectively and there were no false positives in either method. In EOG there were no missed double blinks and the rate of false positives was 3.7% due to a noisy EOG signal that produced 3.9% of false single-blink positives. For this technology, the rate of missing long blinks was 3.1%, mainly confused with single blinks because of an inappropriate duration, and 6.1% of false long-blink positives were all due to a noisy signal.

Neither the technology employed (EOG, VOG, IROG) nor the method of access (double- or single-blink) had a statistically significant effect on accuracy according to the KW test ( $p > 0.5$  in both hypothesis). Nevertheless, in a one-to-one comparison IROG was more accurate than VOG, the former has an accuracy that is higher than the latter ( $p = 0.045$ , KW test). Furthermore, IR-OG was more efficient than the other technologies according to the number of false single-blinks detected and missed long-blinks ( $p < 0.02$  in both cases).

## 2) CP SUBGROUP

RBB started using long blinks as her method of access, but in the end, she was able to control the double blink much better, and this became her preferred method. As we explained in the description of subjects, RBB blinks normally, but when she wants to close both eyes voluntarily, for longer, she does so asymmetrically: her left eye closes after the right one and for a shorter period of time. For this reason, we focused on the voluntary control of her right eye for EOG and IR-OG while we are interesting in seeing the effect of this asymmetry in VOG, which bases its operation on analyzing the average closing/aperture of the two eyes at the same time. For double blinks this asymmetry does not occur or is not perceptible.

In EOG she obtained 100% accuracy with double blinks and a very low percentage with long blinks (28.9%). This was because 57.5% of long blinks were classified as doubles because she opened her right eye slightly during the long blink. There was a small number of incorrectly classified single blinks (1.4%) but a high number of false long blinks (23.8%) due to a noisy signal or actions like laughing. In IR-OG she improved accuracy with long blinks because it seems that this technology is not as sensitive to partial eye aperture during long blinks as EOG (see Figure 16 for an IR signal for an incorrect double blink). However, with IR-OG there was a high percentage of false long (29%) and short blinks (9.7%), most coming from actions like laughing, rapid vertical movements or head movements, all of which produce a change between the relative position of the IR sensors and the eyelids. RBB refused to repeat the experiment with the IR glasses because she felt uncomfortable with them.

With VOG, RBB obtained similar scores in accuracy (above 75%) with both long and double blinks. When the long blink was enabled, the EAR signal showed two steps caused, on the one hand, by RBB not closing both eyes simultaneously and, on the other hand, by the averaging of the left and right EAR signal. The lowest value is associated to both eyes closed and the intermediate value is when just one is closed. Sometimes this signal was incorrectly classified as two long blinks or one double, but with less influence than in EOG. Other false positives were caused by noise in the signal or by laughing, that affected the EAR signal like long blinks; etc. There were similar figures for missing (13%) and false positives (30%) with double blinks mostly caused by a noisy signal or head movements.

MNR tested IR-OG with long blinks in one session. The amount and amplitude of the involuntary movements of her head meant that we decided not to use the glasses anymore to avoid injury. Those movements also made the glasses change position, so the sensors had to be readjusted and the glasses secured in the middle of the session. The low accuracy obtained (56.4%) was due mainly to the high amount of false positives detected for both short and long blinks. These head movements account for 60% of them, given the raw signal a pattern that could be confused with long or short blink. Other false positives were caused by laughing, which changed the relative position between the sensor and the eyelid, in addition to partial eye closure.

The accuracy with long blinks in EOG was very low (37.5%). This was because of the high number of uncontrolled head movements that, with the eye fixed on the computer screen, meant that the ocular dipole moved upwards/downwards, generating an EOG signal that was similar to a long blink. Double-blink detection was more insensitive to uncontrolled movements according to the observed accuracy (95.1%). Here, some false double blinks happened when a short blink was followed by a brief head movement.

MNR preferred using VOG with double blinks with which she obtained an accuracy of 80.7% and none went undetected. Some false positives were due to coughing, which involves closing the eyes or due to a noisy signal. For long blinks, the accuracy worsened because of the high missing rate (36%) and the amount of false positives generated when the VOG was recovered. MNR obtained the highest rate of missing signal, which, in her case, was 30% of the total duration of the experiment.

PLS usually leans over the left side of her wheelchair. As a consequence, the use of any gadget placed on her head was ruled out. This included both the EEG headset and the IR-OG glasses. PLS usually answers simple yes/no questions just by looking upwards for a while to say yes. During two sessions we tried to train her to perform long and double blinks but the latter was very difficult for her because she closes her eyes slowly. For that reason we focused on long blinks. When using EOG the signal associated to the action of saying yes with her eyes was similar to a long blink. This was because when the eye looked upwards, the positive part of the

ocular dipole approached to the upper electrode, generating a positive electrical deviation from the baseline into the EOG signal. The high-pass filter in the circuit made the signal go slowly down towards the baseline even if the eye gaze was kept upwards. As PLS looked at the computer screen again, the electrical signal fell down below the baseline. Therefore, the action of looking upwards and then downwards mimicked the pattern #1 of an EOG long-blink signal (Figure 6). She obtained an accuracy of 90.5% in detecting long blinks, with a percentage of false positives of 5% and 5% of missing long blinks.

To test VOG, and obtain a vertical image of PLS's face, we used an articulated arm attached to the wheelchair, with a directional clamp gripping the external USB camera and allowing its adjustment. The EAR signal remained low when PLS looked at the computer screen and increased when she said 'yes' with her eyes. This behavior was the opposite of we expected for a usual long blink in VOG. Only, involuntary blinks were still characterized by narrow valleys in the EAR signal. Two solutions were possible to adapt VOG to PLS. The first was to invert the EAR signal. The second was to remove the upper temporal constraint of a long blink, so that it could last longer. In fact, the second should also have been applied to the first to allow her more time to do a long blink. With the second solution, a long blink started as PLS began looking at the screen and stopped when she said 'yes'. This simple adjustment in the code achieved an accuracy of 89.4% in detecting long blinks, with a percentage of false positives of 1.7% and with 9.2% of missing long blinks.

## VII. DISCUSSION

The OSHW IR-OG equipment outperforms in accuracy (99.3 %) all similar devices in the reviewed literature and the three other tested technologies when they are used for people without disabilities. The averaged sensitivity in the experiment was 98.2% for that group, which is very close to the 100% obtained in [20] with similar experimental conditions. There were non-significant differences in accuracy between people without disabilities and ALS. For people with CP, with associated uncontrolled head movements, the accuracy dropped drastically due to small displacements, actions that mimicked long blinks (such as laughing), etc. The efficiency of IR-OG has been demonstrated although it needs another more appealing, comfortable and harmless support to host the IR diodes and that are compatible for people wearing corrective glasses. Despite all these issues, it was the preferred wearable technology together with EOG for people without disabilities.

In EOG, the people without disabilities achieved an accuracy of 97.2% with double blinks, which improves similar studies (Table 2) with the same number of electrodes [25], [27] or higher [59], [60]. However, long-blink detection did not obtain very good results (76.5% for people who took part in Exp1, <40% for RBB and MNR and <65% for NTN) as we explained in the results section. This was due to the fact that the EOG signal showed different patterns.

**TABLE 13.** Confusion matrix for the EEG detector when discriminating two types of possible input events using our algorithm.

		Predicted		
		SB	DB	None
SB	745	0	37	
DB	7	614	15	

Figure 17 shows the signals from three different subjects when performing long blinks. The most common EOG signal pattern for long blink is at the top of the figure. The algorithm works quite well for this kind of signal. Nonetheless, for the two others, after applying the derivative filter, the algorithm classifies the long blinks as short for the distance between the N and P waves. To address with this issue and improve the classification results, we could have easily added in the algorithm that a N-P-P sequence is also associated to a long blink. This excludes the detection of the pattern N-P-N, which scarcely appears and its inclusion in the algorithm could endanger the short-blink detection accuracy. Other reasons for the low accuracy were facial gestures, like raising the eyebrow, or moving the ocular globe upwards/downwards, which mimics the long-blink signal.

The commercial EEG headset was the least appealing device and it had to be ruled out in cases in which the subject did not have good control of the head: their need for a headrest meant that they could not wear the headset. The proprietary algorithm did not detect long blinks, only short ones, with an accuracy of 83.3% in people without disabilities, significantly higher than the 50% published in [45]. Our modification of the algorithm used in IR-OG (described in Appendix C) and which we applied to EEG raw data, led to an improvement in results (Table 13). For example, average sensitivity in Table 6 was 89.8%, but with our algorithm this increased to 95.3% (from Table 13,  $745/(745 + 37) = 0.9527$ ). In addition, accuracy also improved from 88% up to 95.8% for global classification, from 83.3% to 94.4% for only short-blink detection and from 85.9% up to 97.2% for double blinks.

Moreover, our algorithm was capable of detecting long blinks. In a brief preliminary study, we observed that most long blinks in the EEG raw signal were accompanied by two N waves (as shown in Figure 18). The first N wave was very close to the P wave and might have made that the algorithm wrongly classify the long blink as short. Hence, the identification of the existence of a second one during a period of time, arbitrarily set at 0.5s, may have benefited the long-blink detection rate. We obtained a sensitivity of 56.4% and an accuracy of 53.5% for long blinks. There were several factors limiting the accuracy. One of them was that not all signals contained the second N wave. In such cases, the algorithm was not able to correctly classify long blinks. Secondly, the search for any additional N wave was limited to 0.5s. This meant that if the long blink lasted longer, the second N waves would appear after the searching time ended, and, therefore, the long blink would be misclassified again. The apparent solution of increasing the time limit has the side effect of delaying the short-blink detection which, in turn, affects the

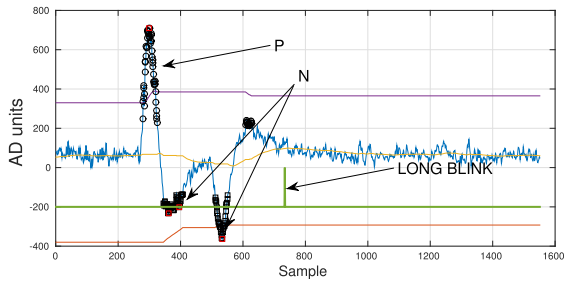


FIGURE 18. Long blink identification. The existence of second N wave during a period of time is used for its identification.

TABLE 14. Percentage of time in which the EAR signal was missing in Exp2.

Name	Tracking lost(%)
MRM	10
MLI	7.6
NTN	0.15
AFL	8.5
RBB	7.2
MNR	30.1
PLS	0.86

double-blink accuracy. To address this situation, the final layers of the algorithm need to be restructured. This could also benefit the long-blink classification for EOG signals.

The favorite interaction method was VOG for people without/with disabilities, for whom it seems that not having to put a device on is preferable. For the correct localization of the face landmarks the subject needs to be facing the camera, in normal lighting, otherwise the algorithm could fail to track the eye correctly, reducing its accuracy. Furthermore, to correctly locate the landmarks initially, the face must be in a vertical position. For some people with severe disabilities this is not possible. To overcome this, we had to tilt the camera until the landmark detection worked. After that, the algorithm was able to keep tracking with certain degree of tolerance to slow yaw, pitch and roll head movements. Table 14 shows the percentage of experiment time in which the EAR signal was missing. As expected, MNR obtained the highest percentage of missing signal time because of the amount, velocity and amplitude of her uncontrolled movements. Those who stayed stiller and looked at the communication board during the experiment got lower percentages, with the exception of AFL, who had a thick nasal canula for breathing. This crossed the face horizontally and might have affected the effectiveness of the tracking.

In optimal conditions, there was an average level of accuracy of 93.4% for people in Exp1 in VOG, which was less than for IR-OG, EOG or EEG - when our algorithm was used - and lower than for some reviewed studies contained in Table 3, excluding [16], [56], [67], [86] which had similar or lower accuracy. The highest accuracy was obtained by methods that, firstly, detected the head and eyes with the Viola-Jones algorithm and, then, applied a median blur filter in the eye area, thresholded the image and counted the pixels [4], [51]. There was no statistically significant difference in accuracy

when using long or double blinks in VOG. However, some double blinks were misinterpreted as long blinks due to the use of a low video sampling rate ( $F_s = 12$  fps) which fused the two blinks signal as a noisy long blink. To overcome this, the video sampling rate needs to be increased, thus shortening frame-processing time. Since video processing requires considerable computational resources, more powerful computers will be needed to execute the algorithm with these time constraints. Other causes limiting accuracy included noisy signals or the subject performing other facial gestures that mimicked the EAR signal (like raising the eyebrow or laughing). To remedy these situations, the algorithm should include certain filtering techniques and analyze more facial landmarks associated, for example, to the lips and the eyebrow. This would help discriminate whether the EAR signal contained a pure blink. The algorithm should also restart the centroids and the processing after the recovery of the tracking to prevent many false positives.

Another topic concerns voluntary blinking and why the realization of winks was ruled out of this study. We thought that it would be easier for subjects to close both eyes at the same time, causing less fatigue and producing continuous lubrication of both eyes, reducing the impact of involuntary blinking. Besides, not all people are capable of winking. In fact, it has been shown that more neural resources are required in winking than in performing voluntary blinks using both eyes at the same time [89]. Excluding EOG, the use of double blinks or long blinks does not influence the accuracy of the technology, although the former have been shown to be faster than the latter. Additionally, in some technologies, long blinks can mimic other facial gestures, apart from blinking, which makes double blinks much robust. However, In spite of the benefits of using double blinks, most users chose the long blink as their method of input.

It is important to highlight that not all people with disabilities can perform voluntary short blinks, close both eyes symmetrically or execute a double blink perfectly. Therefore, any system that works by detecting a voluntary blink of any type, rather than a specific pattern (double or long) would benefit from its accuracy. For example, Figure 16 showed a double blink that was classified as long. The user did not completely open her eyelid between blinks and generated a signal pattern closer to a long blink. Therefore, the system failed to identify the double blink, but succeeded in identifying a voluntary event.

Finally, we could have reduced some false double blinks by not limiting the number of short blinks to two. Sometimes, subjects made more than two blinks, and the third one, together with an involuntary blink produced immediately after it, made a false double blink. To avoid this, the final state machine should consider a burst of variable short blinks as a single voluntary event.

### VIII. CONCLUSIONS AND FUTURE WORK

In this work we have presented several technologies for accessing a computer using voluntary blinks. Several

inexpensive open-source hardware platforms and algorithms have been developed. Most of them outperformed their counterparts in the scientific literature in terms of accuracy. Moreover, we have proposed an algorithm which improves the detection of blinking in a commercial EEG headset.

People with disabilities in their common environments obtained similar performances to people without disabilities. Results were slightly better on average for people with ALS in all technologies and input methods than for those with CP due to the lack of involuntary movements, greater voluntary control and higher intellectual capabilities. The use of long blinks was preferred by most people despite double blinks being faster, more insensitive to other facial gestures and more accurate when EOG was used.

VOG was the most popular technology even though it did not obtain the best results in accuracy. It seems that its greater ease of use outweighed other technical considerations. In the future, we will continue to work on VOG, improving the algorithm that detects the landmarks to make it more independent of head movements and signal noise. Furthermore, the algorithm also needs to be improved to avoid false positives when eye tracking is lost.

## APPENDIX A LONG-, SHORT-BLINK DETECTION BASED ON AN IR CIRCUIT

### A. HARDWARE

Figure 19 shows the schematics of the Arduino shield that was implemented. It contains: a) a transistor, controlled by a digital output, that allows the infrared emitter to be turned on/off; b) a phototransistor that converts the reflected IR into current, which is sent to a low-pass filter preamplifier with a gain of 10 and a cutoff frequency of 22.6 Hz; c) a passive high-pass filter with a cutoff frequency of 2.3 Hz and d) an adjustable amplifier that sets the output signal to a range appropriate for digitalization. A virtual ground circuit is also included. Additionally, a frame hosting the IR elements has also been developed. The schematics, the 3D model of the frames and the Arduino software can be downloaded from the following url: <https://github.com/aljemoca/BlinkingIROG>

### B. BLINK DETECTION ALGORITHM FOR IR-OG

The software has been split into 5 different layers distributed like in a pipeline: the lowest, or hardware layer, receives data from the analog to digital converter (ADC) while the top layer identifies the short and long blinks. Each layer acts as a unit processing receiving input data and sending results out toward the next layer in the pipeline. We used the open-source library described in [53] to build the application (library LBSP available at <https://lbsp.sourceforge.io>).

#### 1) LAYER 1: HARDWARE LAYER

This layer guarantees the acquisition at a fixed rate of 250 Hz and is completely implemented in the LBSP library.

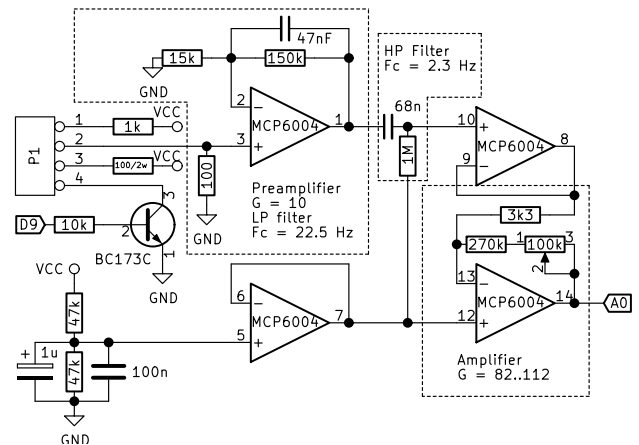


**FIGURE 19.** The IR detector/generator circuit. Infrared leds are connected to the circuit through P1. The input signal is firstly amplified and low pass filtered in the preamplifier stage. Then a high pass filter and a final amplifier with adjustable gain generates the signal to be digitalized at a rate of 250Hz.

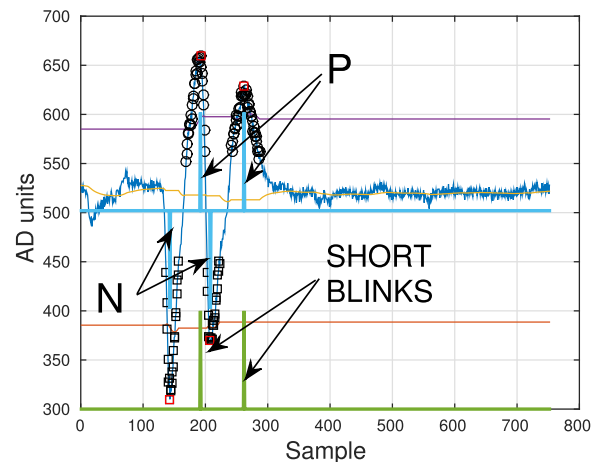


**FIGURE 20.** A signal associated with a double blink captured by the IR circuit. It contains two negative and positive waves. The centroids of the classifier are also shown (thin purple, orange and red lines). Samples classified as belonging to the negative/positive centroids are shown with squares and circles respectively. The position of the extrema in each wave is colored in red and the output of the waves identification layer is in a thick blue line. Note that the position of N, P pulses has been corrected with the *delaymax* variable.

#### 2) LAYER 2: FILTERING

Data coming from the hardware layer might contain noise due to room lighting. In Europe the frequency of power lines is 50Hz, so an IR interference can be found at 100Hz. A low pass digital filter, with Q15 coefficients  $h = [691, 3358, 7509, 9647, 7509, 3358, 691]/32764$ , which make a gain of -98dB at 100Hz, was implemented.

#### 3) LAYER 3: CLASSIFIER

Here, data is classified into three main categories: negative, baseline and positive. It contains an adaptive K-means algorithm that classifies data according to the distance to three centroids, which, in turn, are being continuously adjusted as well (Figure 20). More details about how this layer 3 algorithm works can be found in [52].

The procedure is summarized in Algorithm 1. It uses an input variable, *in*, an internal matrix, *centroid<sub>j</sub>* (where  $j = 1 \dots N_{cent}$ ) and an output, *out*, that returns 0 when the sample belongs to the baseline and a negative/positive value if the sample is below/above the baseline. Each variable is updated whenever a new sample is received in the layer.

Several constants parametrize the algorithm: number of centroids  $N_{cent} = 3$ ; an arbitrary weight for updating the centroids,  $L_c = 32$ ; and the bias = 512, that removes the virtual ground and sets the baseline roughly to zero, enabling the use of signed integers.

---

**Algorithm 1** The Classification Layer Algorithm.
 

---

```

1: Parameters:  $N_{cent} = 3, L_c = 32, \text{bias} = 512$ 
2:
3: Input: in
4: Output: out
5: Internal: centroidj;  $j = 1..N_{cent}$ 
6:
7:  $\text{in} = \text{in} - \text{bias}$  //To remove DC bias
8:  $[d_j, \text{pos}] = \min_j(|\text{in} - \text{centroid}_j|)$   $j = 1..N_{cent}$ 
9: if  $d_j > 2$  then
10:    $\text{centroid}_{\text{pos}} = \frac{(L_c-1) \times \text{centroid}_{\text{pos}} + \text{in}}{L_c}$ 
11: end if
12:  $\text{out} = \text{pos} - 2$ 

```

---

#### 4) LAYER 4: WAVES IDENTIFICATION

This layer receives the signal, *in*, the classification results of lower layer, *clas*, and outputs an integer, *out* = [-1, 0, 1], identifying groups of samples belonging to the N, P waves or the baseline.

To do that, we have implemented a two-state finite state machine (FSM), including an area estimation procedure and the search of the minimum/maximum samples position in respective N/P waves (Algorithm 2). In its initial state, the FSM waits for a non-baseline sample to come. When it does, the integration process, to estimate the area of the wave, and the search for the wave extrema is initiated. On the one hand, the calculation of the area helps to filter small amounts of samples that can be found inside the wave that belong to the opposite class. On the other hand, by searching for the maximum/minimum extrema in the wave, we get a steadier feature for distinguishing short blinks from long ones than if we used other features such as the position of the first sample associated with the N and P waves, which could be more influenced by signal noise.

In the next state, the FSM keeps on calculating the area and the extrema as long as the input does not belong to the baseline. Otherwise, the FSM assesses the area, outputs its sign and returns to the initial state. The *delaymax* variable contains the position of the extrema from the sample in which this layer signaled an N or P wave. Fig. 20 illustrates the operation of this layer in cyan and the position of the extrema in red.

---

**Algorithm 2** The Waves Identification Algorithm
 

---

**Input:** *in*, *clas*  
**Output:** *out*, *delaymax*  
**Internal:** *state*, *area*, *maxim*, *delaymax*

```

N = -1
P = 1
out = 0
maxim = 0
area = 0

if state == 0 then
  if clas != 0 then
    area = area + in
    state = 1
    if  $\text{abs}(\text{in}) > \text{maxim}$  then
      maxim =  $\text{abs}(\text{in})$ ;
      delaymax = 0;
    end if
  end if
end if
if state == 1 then
  if clas != 0 then
    area = area + in
    delaymax = delaymax + 1
    if  $\text{abs}(\text{in}) > \text{maxim}$  then
      maxim =  $\text{abs}(\text{in})$ ;
      delaymax = 0;
    end if
  else
    if area <= 0 then
      out = N
    else
      out = P
    end if
    area = 0
    state = 0
    maxim = 0
  end if
end if

```

---

#### 5) LAYER 5: LONG AND SHORT BLINK IDENTIFICATION

A long, short blink is a sequence of an N pulse followed by a P pulse in a period of time. The time lapse (or number of samples), between extrema positions of both N and P waves, allows us to distinguish between them.

To do that, this level contains a two-state FSM with an internal variable, *time*, that counts the number of samples between waves extrema. The input variables *posminN* and *posmaxP* are the *delaymax* output for the lower layer and help detect the position of the extrema with respect to the current sample. We considered an N-P sequence happening in a period of  $T_{sb} < 98$  samples, as a short blink. Greater values will be considered as long blinks but with a maximum

**Algorithm 3** The Long and Short Blink Identification Algorithm

```

1: Input: in, posminN, posmaxP
2: Output: out
3: Internal: state, time
4:
5: ShortBlink = 1
6: LongBlink = 2
7: Tsb = 98
8: Tlb = 2*Fs
9: out = 0
10: if state == 0 then
11:   if in == N then
12:     time = posminN
13:     state = 1
14:   end if
15: end if
16: if state == 1 then
17:   time = time+1
18:   if in == N then
19:     time =posminN
20:   end if
21:   if in == P then
22:     time = time – posmaxP
23:     if time < Tsb then
24:       out = ShortBlink
25:     end if
26:     if time > Tsb AND time < Tlb then
27:       out = LongBlink
28:     end if
29:     state = 0
30:   end if
31: end if

```

limit of  $T_{sb} < T_{lb} < 2 * F_s = 500$  samples. Algorithm 3 describes in detail the procedure and the green thick line in Figure 20 shows this layer’s output, indicating that there were two short blinks.

**APPENDIX B**  
**LONG AND SHORT BLINK DETECTION BASED ON AN EOG**  
**A. HARDWARE**

The circuit is based on a three-electrode single-supply bio-amplifier published in [71], [84] and Figure 21 show its schematic layout. Two electrodes (EOG+, EOG-) are used to capture the bioelectrical signal while the third one (REF) reduces power-line interference. The REF electrode is driven by an operational amplifier through high impedance resistors that limit the current injected towards the subject. The input voltage of this amplifier comes from the output of another amplifier working as virtual ground and creating a potential, with a low impedance, between GND and VCC. The value of such a potential is set by a voltage divider.

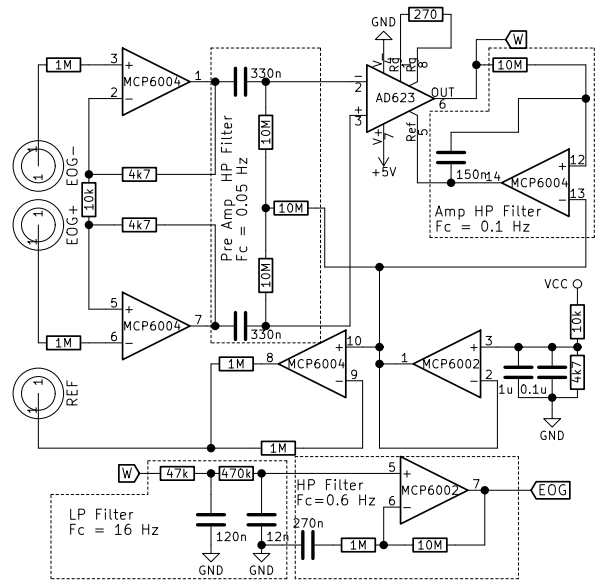


**FIGURE 21.** The EOG circuit based on a modification of an ECG circuit [71]. It uses three electrodes to measure the bioelectrical activity and reduce power line interference. The final stage contains a band-pass filter with a frequency range between 0.6-16Hz.

The first stage in amplifying the EOG biopotential are formed by two operational amplifiers in differential mode. This stage has high input impedance and low gain, which prevents the bioamplifier from becoming saturated by the electrodes half-cell potential difference. Then, a differential high pass filter, built with two capacitors and a T-resistor network, allows DC bias to be removed, due to electrode half-cell potential, without significant CMRR degradation. In the next stage, a low cost instrumentation amplifier, with a high CMRR, amplifies the biopotential significantly. Its output does not contain a DC component thanks to an inverter high-pass filter that feedbacks instrumentation amplifier output to its own instrumentation amplifier. Then, a double-pole low-pass filter smooths the instrumentation amplifier output and reduces the power line interference. Finally, a high-pass filter with a gain of 11 is implemented with one operational amplifier. The circuit has a frequency response ranging from 0.6 Hz up to 16Hz and the schematic, together with the Arduino software, can be downloaded from the link: <https://github.com/aljemoca/BlinkingEOG>.

**B. ALGORITHM**

Firstly, a notch filter, tuned to 50 Hz, is applied to reduce power line interference Eq. 2.

$$H(z) = \frac{z^2 - 0.618z + 1}{z^2 - 0.601z + 0.92} \quad (2)$$

Then, the derivative of the signal is obtained through a Savitzky-Golay filter with length 21 and order 3 with coefficients [0.0231, 0.0028, -0.0119, -0.0215, -0.0267, -0.0280, -0.0262, -0.0219, -0.0157, -0.0081, 0.0000,



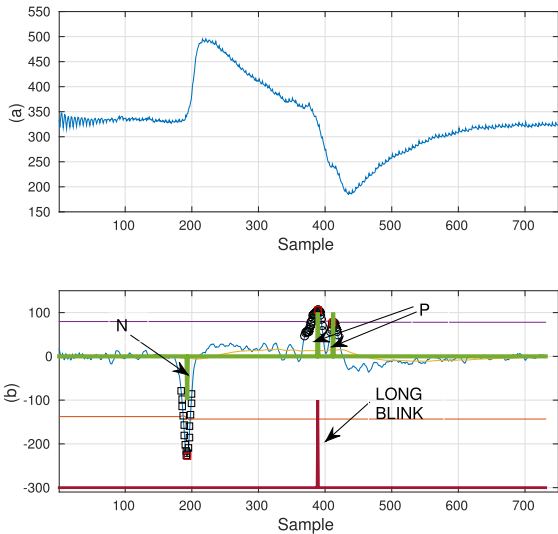


**FIGURE 22.** (a) An EOG signal associated with a long blink. This signal has been filtered to remove power line interference. (b) A Savitzky-Golay [78] filter is then applied to obtain the derivative of the signal and remove the wandering. The derivative signal contains a negative and a positive wave. The centroids of the classifier are also shown. The samples classified as belonging to the lowest/highest centroid are shown with squares or circles respectively. The output of the waves identification layer is also shown.

0.0081, 0.0157, 0.0219, 0.0262, 0.0280, 0.0267, 0.0215, 0.0119, -0.0028, -0.0231].

After this filter, the signal contains positive and negative waves in a similar way to the one obtained by the IR circuit. For this reason, the algorithm to detect the short or long blinks are basically the same as described above in Algorithm 1, although with the parameter *bias* set to 0. The rest of the layers in the algorithm are identical. We used the open-source library described in [53] to build the filters and the rest of the layers.

Figure 22 shows the original EOG signal (a), its derivative (b), the three centroids, the samples classified as belonging to N waves (squares) or P waves (circles). Notice that, in this case, there are two P waves and only the first one is used to determine the time between the N-P waves. If this time exceeds a preset limit, the blink is identified as long, otherwise as short.

**APPENDIX C  
SHORT BLINK DETECTION BASED ON AN EEG HEADSET**

As shown in Figure 6, EEG signals are quite similar to EOG apart from the fact that a short blink is defined by a sequence of P-N waves instead of the N-P pair. We use Algorithm 1 with the parameter *bias* set to 0 and with  $L_c = 64$ . Algorithm 2 was used for the waves' identification and Algorithm 3 to identify the type of blink, but with the P and N constants swapped. Matlab routines can be downloaded from <https://github.com/aljemoca/BinkingEEG>.

**Algorithm 4** The Blink Detector Algorithm for VOG

**Input:** in //The classification result  
**Output:** out  
**Internal:** state, length

```

N = -1
out = 0
length = 0

if state == 0 then
  if in == N then
    length = length + 1
    state = 1
  end if
end if
if state == 1 then
  if in == N then
    length = length + 1;
  else
    out = LongBlink
  end if
  if length == 0; state = 0;
end if
end if

```

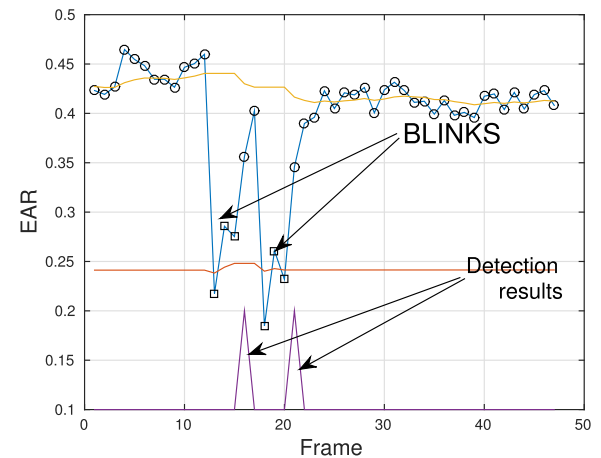


**FIGURE 23.** Typical EAR signal for double-blink actions. Two centroids are used to classify samples belonging to eye actions (squares) or not (circles). The final result is also shown.

**APPENDIX D  
LONG AND SHORT BLINK DETECTION BASED ON VOG**

We addressed the detection of blinks from VOG using the same previous idea but from a slightly different perspective. We were able to adapt the algorithm used in IR-OG to EOG by applying a Savitzky-Golay filter to estimate the derivative of the input signal and generate a new signal with a similar two N-P sequence like the IR-OG signal. Since the EAR signal

**Algorithm 5** The Voluntary Blinking Detection Algorithm. It is Based on Searching for Long Blinks or a Sequence of Two Short Blinks in a Period of Time.

```

1: Input: in
2: Output: out
3: Internal: state, time
4:
5: Timeout = 1.2*Fs
6: out = 0
7: if in == LongBlink then
8:   state = 0
9:   out = out OR 2
10: else
11:   if state == 0 then
12:     if in == ShortBlink then
13:       out = out OR 1
14:       state=1
15:       time=0
16:     end if
17:   end if
18:   if state == 1 then
19:     time ++
20:     if time > Timeout then
21:       state=0
22:     end if
23:     if in == ShortBlink then
24:       state=0
25:       out = out OR 5
26:     end if
27:     if in == LongBlink then
28:       state=0
29:       out = out OR 3
30:     end if
31:   end if
32: end if

```

is noisy and the number of samples is fairly small, 12 per second, applying a filter in the same way to obtain a such two-wave signal is not feasible.

The EAR signal is sent directly to a two-centroid K-means adaptive classifier (Algorithm 4). Samples are identified as belonging to a baseline or a blink (circles and squares in Figure 23 respectively). Additionally, Algorithm 1 was configured with the following parameters:  $N_{cent} = 2$ ,  $L_c = 8$  and bias = 0. Then, the blink samples were grouped together and, according to their duration, identified as short or long blinks.

The project can be downloaded from the following link: <https://github.com/manmermon/CamBlinkDetector>

## APPENDIX E VOLUNTARY BLINK DETECTION

This is the last layer in the processing pipeline and common for any employed technology. It receives short blinks (1), long blinks(2) or none (0) from downer layers and decides the willfulness of the subject. In this sense, any sequence of

two short blinks in a lapse of time (set to Timeout =  $1.2 * F_s$  samples) or a long blink alone are considered as voluntary blinks.

A two-state FSM was set up to implement the functionality of this layer (Algorithm 5). Initially, the machine starts from a state in which it is waiting for a long or short blink to come. If a long blink is detected, the output is automatically activated and the machine continues in the same state. If a short blink is detected, the machine moves to another state and starts a timer. In this new state, if a long blink is received or a short blink appears before the timer expires the output is activated. Otherwise the machine stays in this state for a period of time that equals Timeout, before going back to the first state.

## ACKNOWLEDGMENT

The authors would like to thank the following: Alejandro Gallardo for the implementation of the Arduino shields; the participants, for actively cooperating in the development of this work and especially AFL, MLI, MNR, MRN, NTN, PLS and RBB for their incredible enthusiasm, willingness and patience; the staff of two organizations we visited *Colegio Mercedes Sanroma* and *ELA Andalucía*, particularly Raquel Delgado and Setefilla Álvarez, for helping and supporting us in selecting the candidates, for sharing their years of experience and for facilitating the resources needed to carry out the experiment; Patrick Partridge who thoroughly revised the manuscript; Alba Molina, who drew an amazing and beautiful picture of a woman's eye when she was only thirteen; and finally the anonymous reviewers for their useful suggestions.

## CONFLICT OF INTEREST

The authors declare no conflict of interest.

## REFERENCES

- [1] M. Abo-Zahhad, S. M. Ahmed, and S. N. Abbas, "A novel biometric approach for human identification and verification using eye blinking Signal," *IEEE Signal Process. Lett.*, vol. 22, no. 7, pp. 876–880, Jul. 2015.
- [2] R. Ahmad and J. N. Borole, "Drowsy driver identification using eye blink detection," *Int. J. Comput. Sci. Inf. Technol.*, vol. 6, no. 1, pp. 270–274, Jan. 2015.
- [3] A. Asthana, S. Zafeiriou, S. Cheng, and M. Pantic, "Incremental face alignment in the wild," in *Proc. IEEE Conf. Comput. Vis. Pattern Recognit.*, Jun. 2014, pp. 1859–1866.
- [4] C. D. N. Ayudhya and T. Srinark, "A method for real-time eye blink detection and its application," in *Proc. 6th Int. Joint Conf. Comput. Sci. Softw. Eng. (JCSSE)*, 2009, pp. 1–6.
- [5] G. Bauer, F. Gerstenbrand, and E. Rimpl, "Varieties of the locked-in syndrome," *J. Neurol.*, vol. 221, no. 2, pp. 77–91, 1979.
- [6] A. R. Bentivoglio, S. B. Bressman, E. Cassetta, D. Carretta, P. Tonali, and A. Albanese, "Analysis of blink rate patterns in normal subjects," *Movement Disorders*, vol. 12, no. 6, pp. 1028–1034, 1997.
- [7] P. Biswas and P. Langdon, "A new interaction technique involving eye gaze tracker and scanning system," in *Proc. Conf. Eye Tracking South Africa*, 2013, pp. 67–70.
- [8] L. Burton, W. Albert, and M. Flynn, "A comparison of the performance of webcam vs. infrared eye tracking technology," in *Proc. Hum. Factors Ergonom. Soc. Annu. Meeting*, vol. 58. Los Angeles, CA, USA: SAGE, 2014, pp. 1437–1441.
- [9] F. L. Castro, "Class I infrared eye blinking detector," *Sens. Actuators A, Phys.*, vol. 148, no. 2, pp. 388–394, 2008.

- [10] M. Challagundla, K. Y. Reddy, and N. H. Vardhan, "Automatic motion control of powered wheel chair by the movements of eye blink," in *Proc. Int. Conf. Adv. Commun. Control Comput. Technol. (ICACCCT)*, May 2014, pp. 1003–1007.
- [11] M. Chau and M. Betke, "Real time eye tracking and blink detection with USB cameras," Dept. Comput. Sci., Boston Univ., Boston, MA, USA, Tech. Rep. 2005-12, 2005.
- [12] E. Dalmajier, "Is the low-cost EyeTribe eye tracker any good for research?" *PeerJ PrePrints*, vol. 2, 2014, Art. no. e585v1. doi: 10.7287/peerj.preprints.585v1.
- [13] R. Das, D. Chatterjee, D. Das, A. Sinharay, and A. Sinha, "Cognitive load measurement—A methodology to compare low cost commercial eeg devices," in *Proc. Int. Conf. Adv. Comput., Commun. Inform. (ICACCI)*, Sep. 2014, pp. 1188–1194.
- [14] A. Dementyev and C. Holz, "Dualblink: A wearable device to continuously detect, track, and actuate blinking for alleviating dry eyes and computer vision syndrome," *Proc. ACM Interact. Mobile Wearable Ubiquitous Technol.*, vol. 1, no. 1, pp. 1:1–1:19, Mar. 2017.
- [15] M. Divjak and H. Bischof, "Eye blink based fatigue detection for prevention of computer vision syndrome," in *Proc. MVA*, 2009, pp. 350–353.
- [16] T. Drutarovsky and A. Fogelton, "Eye blink detection using variance of motion vectors," in *Proc. Eur. Conf. Comput. Vis.* Springer, 2014, pp. 436–448.
- [17] P. Ekman and W. V. Friesen, *Facial Action Coding System: Manual*, vols. 1–2. Washington, DC, USA: Consulting Psychologists Press, 1978.
- [18] A. E. Emery, F. Muntoni, and R. C. Quinlivan, *Duchenne Muscular Dystrophy*. Oxford, U.K.: OUP, 2015.
- [19] S. Fager, D. Beukelman, M. Friede-Oken, T. Jakobs, and J. Baker, "Access interface strategies," *Assist. Technol.*, vol. 24, no. 1, pp. 25–33, 2012.
- [20] A. Frigerio, T. A. Hadlock, E. H. Murray, and J. T. Heaton, "Infrared-based blink-detecting glasses for facial pacing: Toward a bionic blink," *JAMA Facial Plastic Surg.*, vol. 16, no. 3, pp. 211–218, 2014.
- [21] T. Gandhi, M. Trikha, J. Santhosh, and S. Anand, "Development of an expert multitask gadget controlled by voluntary eye movements," *Expert Syst. Appl.*, vol. 37, no. 6, pp. 4204–4211, 2010.
- [22] L. García, R. Ron-Angevin, B. Loubière, L. Renault, G. Le Masson, V. Lespinet-Najib, and J. M. André, "A comparison of a brain-computer interface and an eye tracker: Is there a more appropriate technology for controlling a virtual keyboard in an als patient?" in *Proc. Int. Work-Confer. Artif. Neural Netw.*, 2017, pp. 464–473.
- [23] J. Gips, P. DiMattia, F. X. Curran, and P. Olivieri, "Using EagleEyes—An electrodes based device for controlling the computer with your eyes—To help people with special needs," in *Proc. 5th Int. Conf. Comput. Helping People Special Needs (ICCHP)*, Munich, Germany, 1996, pp. 77–83.
- [24] K. Grauman, M. Betke, J. Gips, and G. R. Bradski, "Communication via eye blinks-detection and duration analysis in real time," in *Proc. Proc. IEEE Comput. Soc. Conf. Comput. Vis. Pattern Recognit. (CVPR)*, vol. 1, Dec. 2001, pp. 1–2.
- [25] X. Guo, W. Pei, Y. Wang, Y. Chen, H. Zhang, X. Wu, X. Yang, H. Chen, Y. Liu, and R. Liu, "A human-machine interface based on single channel EOG and patchable sensor," *Biomed. Signal Process. Control*, vol. 30, pp. 98–105, Sep. 2016.
- [26] S. Han, S. Yang, J. Kim, and M. Gerla, "EyeGuardian: A framework of eye tracking and blink detection for mobile device users," in *Proc. 12th Workshop Mobile Comput. Syst. Appl.*, 2012, pp. 1–6.
- [27] S. He and Y. Li, "A Single-channel EOG-based Speller," *IEEE Trans. Neural Syst. Rehabil. Eng.*, vol. 25, no. 11, pp. 1978–1987, Nov. 2017.
- [28] M. J. C. Hidecker, N. Paneth, P. L. Rosenbaum, R. D. Kent, J. Lillie, J. B. Eulenberg, K. E. N. Chester, Jr., B. Johnson, L. Michalsen, M. Evatt, and K. Taylor, "Developing and validating the communication function classification system for individuals with cerebral palsy," *Develop. Med. Child Neurol.*, vol. 53, no. 8, pp. 704–710, 2011.
- [29] J. Hori, K. Sakano, and Y. Saitoh, "Development of a communication support device controlled by eye movements and voluntary eye blink," *IEICE Trans. Inf. Syst.*, vol. 89, no. 6, pp. 1790–1797, 2006.
- [30] R. J. Jacob and K. S. Karn, "Eye tracking in human-computer interaction and usability research: Ready to deliver the promises," in *The Mind's Eye*. Amsterdam, The Netherlands: Elsevier, 2003, pp. 573–605.
- [31] M. Kassner, W. Patera, and A. Bulling, "Pupil: An open source platform for pervasive eye tracking and mobile gaze-based interaction," in *Proc. ACM Int. Joint Conf. Pervasive Ubiquitous Comput., Adjunct Publication*, 2014, pp. 1151–1160.
- [32] I. Käthner, A. Kübler, and S. Halder, "Comparison of eye tracking, electrooculography and an auditory brain-computer interface for binary communication: A case study with a participant in the locked-in state," *J. Neuroeng. Rehabil.*, vol. 12, no. 1, p. 76, 2015.
- [33] M. R. Kim and G. Yoon, "Control signal from EOG analysis and its application," *World Acad. Sci., Eng. Technol., Int. J. Elect., Electron. Sci. Eng.*, vol. 7, no. 10, pp. 830–834, 2013.
- [34] K. Kothe, *Lab Streaming Layer (LSL)*. Accessed: Jul. 18, 2018. [Online]. Available: <https://github.com/sccn/labstreaminglayer>
- [35] N. Kourkoumelis and M. Tzaphlidou, "Eye safety related to near infrared radiation exposure to biometric devices," *Sci. World J.*, vol. 11, pp. 520–528, Nov. 2011.
- [36] A. Królak and P. Strumillo, "Eye-blink detection system for human-computer interaction," *Universal Access Inf. Soc.*, vol. 11, no. 4, pp. 409–419, 2012.
- [37] M. Lalonde, D. Byrns, L. Gagnon, N. Teasdale, and D. Laurendeau, "Real-time eye blink detection with GPU-based SIFT tracking," in *Proc. 4th Can. Conf. Comput. Robot Vis. (CRV)*, May 2007, pp. 481–487.
- [38] D. Li and D. J. Parkhurst, "openEyes: An open-hardware open-source system for low-cost eye tracking," *J. Mod. Opt.*, vol. 53, no. 9, pp. 1295–1311, 2006.
- [39] Y. Li, S. He, Q. Huang, Z. Gu, and Z. L. Yu, "A EOG-based switch and its application for 'start/stop' control of a wheelchair," *Neurocomputing*, vol. 275, pp. 1350–1357, Jun. 2018.
- [40] Z. R. Lugo, M.-A. Bruno, O. Gosseries, A. Demertzi, L. Heine, M. Thonnard, V. Blandin, F. Pellas, and S. Laureys, "Beyond the gaze: Communicating in chronic locked-in syndrome," *Brain Injury*, vol. 29, no. 9, pp. 1056–1061, 2015.
- [41] Z. Lv, C. Zhang, B. Zhou, X. Gao, and X. Wu, "Design and implementation of an eye gesture perception system based on electrooculography," *Expert Syst. Appl.*, vol. 91, pp. 310–321, Jan. 2018.
- [42] I. S. MacKenzie and B. Ashtiani, "BlinkWrite: Efficient text entry using eye blinks," *Universal Access Inf. Soc.*, vol. 10, no. 1, pp. 69–80, 2011.
- [43] A. Maffei and A. Angrilli, "Spontaneous eye blink rate: An index of dopaminergic component of sustained attention and fatigue," *Int. J. Psychophysiol.*, vol. 123, pp. 58–63, Jan. 2018.
- [44] A. A. Mange, A. V. Choudhari, and S. Prasad, "Gaze and blinking base human machine interaction system," in *Proc. IEEE Int. Conf. Comput. Intell. Comput. Res. (ICIC)*, Dec. 2015, pp. 1–4.
- [45] R. Maskeliunas, R. Damasevicius, I. Martisius, and M. Vasiljevas, "Consumer-grade EEG devices: Are they usable for control tasks?" *PeerJ*, vol. 4, p. e1746, Mar. 2016.
- [46] D. McDuff, A. Mahmoud, M. Mavadati, M. Amr, J. Turcot, and R. E. Kaliouby, "AFFDEX SDK: A cross-platform real-time multi-face expression recognition toolkit," in *Proc. CHI Conf. Extended Abstr. Hum. Factors Comput. Syst. (CHI EA)*, 2016, pp. 3723–3726.
- [47] D. J. McFarland, W. A. Sarnacki, and J. R. Wolpaw, "Brain-computer interface (BCI) operation: Optimizing information transfer rates," *Biol. Psychol.*, vol. 63, no. 3, pp. 237–251, Jul. 2003.
- [48] D. Medine. (2016). *Labstreaminglayer*. [Online]. Available: <https://github.com/sccn/labstreaminglayer/wiki>
- [49] E. Missimer and M. Betke, "Blink and wink detection for mouse pointer control," in *Proc. 3rd Int. Conf. Pervasive Technol. Rel. Assistive Environ. (PETRA)*, New York, NY, USA, 2010, pp. 23:1–23:8.
- [50] G. Mohammadi, J. Shanbehzadeh, and H. Sarrafzadeh, "A fast and adaptive video-based method for eye blink rate estimation," *Int. J. Adv. Comput. Res.*, vol. 5, no. 19, Jun. 2015.
- [51] A. P. A. A. Mohammed, "Efficient eye blink detection method for disabled-helping domain," *Eye*, vol. 10, no. (P1), p. P2, 2014.
- [52] A. Molina, J. Guerrero, I. Gómez, and M. Merino, "A new multisensor software architecture for movement detection: Preliminary study with people with cerebral palsy," *Int. J. Hum.-Comput. Stud.*, vol. 97, pp. 45–57, Jan. 2017.
- [53] A. J. Molina-Cantero, J. A. Castro-García, C. Lebrato-Vázquez, I. M. Gómez-González, and M. Merino-Monge, "Real-time processing library for open-source hardware biomedical sensors," *Sensors*, vol. 18, no. 4, p. 1033, 2018.
- [54] A. J. Molina-Cantero, J. Guerrero-Cubero, I. M. Gómez-González, M. Merino-Monge, and J. I. Silva-Silva, "Characterizing computer access using a one-channel eeg wireless sensor," *Sensors*, vol. 17, no. 7, p. 1525, 2017.
- [55] A. J. M. Cantero, I. M. G. González, O. R. Romero, and M. M. Monge, "A flexible, open, multimodal system of computer control based on infrared light," *Int. J. Latest Trends Comput.*, vol. 2, no. 4, pp. 498–507, 2011.
- [56] T. Morris, P. Blenkhorn, and F. Zaidi, "Blink detection for real-time eye tracking," *J. Netw. Comput. Appl.*, vol. 25, no. 2, pp. 129–143, Apr. 2002.

- [57] K. Mukherjee and D. Chatterjee, "Augmentative and alternative communication device based on eye-blink detection and conversion to morse-code to aid paralyzed individuals," in *Proc. Int. Conf. Commun., Inf. Comput. Technol. (ICCICT)*, Jan. 2015, pp. 1–5.
- [58] K. Mukherjee, R. Karmakar, and S. Das, "Effective estimation of driver drowsiness based on eye status detection and analysis," in *Proc. Int. Conf. Devices, Circuits Commun. (ICDCCom)*, Sep. 2014, pp. 1–4.
- [59] H. Mulam and M. Mudigonda, "A novel method for recognizing eye movements using NN classifier," in *Proc. 3rd Int. Conf. Sens., Signal Process. Secur. (ICSSS)*, May 2017, pp. 290–295.
- [60] M. Nakanishi, Y. Mitsukura, Y. Wang, Y.-T. Wang, and T.-P. Jung, "Online voluntary eye blink detection using electrooculogram," in *Proc. Int. Symp. Nonlinear Theory Appl.*, Palma, Spain, 2012, pp. 1–4.
- [61] L. F. Nicolas-Alonso and J. Gomez-Gil, "Brain computer interfaces, a review," *Sensors*, vol. 12, no. 2, pp. 1211–1279, 2012.
- [62] R. Palisano, P. Rosenbaum, S. Walter, D. Russell, E. Wood, and B. Galuppi, "Development and reliability of a system to classify gross motor function in children with cerebral palsy," *Develop. Med. Child Neurol.*, vol. 39, no. 4, pp. 214–223, 1997.
- [63] F. J. Parada, D. Wyatte, C. Yu, R. Akavipat, B. Emerick, and T. Busey, "ExpertEyes: Open-source, high-definition eyetracking," *Behav. Res. Methods*, vol. 47, no. 1, pp. 73–84, 2015.
- [64] S.-W. Park, Y.-L. Yim, S.-H. Yi, H.-Y. Kim, and S.-M. Jung, "Augmentative and alternative communication training using eye blink switch for locked-in syndrome patient," *Ann. Rehabil. Med.*, vol. 36, no. 2, pp. 268–272, 2012.
- [65] A. Pasarica, R. G. Bozomitu, V. Cehan, and C. Rotariu, "Eye blinking detection to perform selection for an eye tracking system used in assistive technology," in *Proc. IEEE 22nd Int. Symp. Design Technol. Electron. Packag. (SIITME)*, Oct. 2016, pp. 213–216.
- [66] E. Pasqualotto, T. Matuz, S. Federici, C. A. Ruf, M. Bartl, M. O. Belardinelli, N. Birbaumer, and S. Halder, "Usability and workload of access technology for people with severe motor impairment: A comparison of brain-computer interfacing and eye tracking," *Neurorehabil. Neural Repair*, vol. 29, no. 10, pp. 950–957, 2015.
- [67] L. Pauly and D. Sankar, "Non intrusive eye blink detection from low resolution images using HOG-SVM classifier," *Int. J. Image, Graph. Signal Process.*, vol. 8, no. 10, p. 11, 2016.
- [68] C. G. Pinheiro, E. L. Naves, P. Pino, E. Losson, A. O. Andrade, and G. Bourhis, "Alternative communication systems for people with severe motor disabilities: A survey," *Biomed. Eng. Online*, vol. 10, no. 1, p. 31, 2011.
- [69] O. Polacek, A. J. Sporka, and P. Slavik, "Text input for motor-impaired people," *Universal Access Inf. Soc.*, vol. 16, no. 1, pp. 51–72, 2017.
- [70] P. Polatsek, "Eye blink detection," in *Proc. Conf. IIT.SRC*, 2013, pp. 1–8.
- [71] R. Quesada-Tabares, J. Alberto Molina-Cantero, I. Gomez-González, M. Merino-Monge, A. J. Castro-Garcia, and R. Cabrera-Cabrera, "Emotions detection based on a single-electrode EEG device," in *Proc. 4th Int. Conf. Physiol. Comput. Syst.*, vol. 1, 2017, pp. 89–95.
- [72] R. Sharma, S. Hicks, C. M. Berna, C. Kennard, K. Talbot, and M. R. Turner, "Oculomotor dysfunction in amyotrophic lateral sclerosis: A comprehensive review," *Arch. Neurol.*, vol. 68, no. 7, pp. 857–861, 2011.
- [73] S. B. Ryan, K. L. Detweiler, K. H. Holland, M. A. Hord, and V. Bracha, "A long-range, wide field-of-view infrared eyeblink detector," *J. Neurosci. Methods*, vol. 152, nos. 1–2, pp. 74–82, 2006.
- [74] J. S. Agustin, H. Skovsgaard, E. Mollenbach, M. Barret, M. Tall, D. W. Hansen, and J. P. Hansen, "Evaluation of a low-cost open-source gaze tracker," in *Proc. Symp. Eye-Tracking Res. Appl.*, 2010, pp. 77–80.
- [75] C. Sankar and N. Mundkur, "Cerebral palsy-definition, classification, etiology and early diagnosis," *Indian J. Pediatrics*, vol. 72, no. 10, pp. 865–868, Oct. 2005.
- [76] T. Santini, W. Fuhl, D. Geisler, and E. Kasneci, "EyeRecToo: Open-source software for real-time pervasive head-mounted eye tracking," in *Proc. 12th Int. Joint Conf. Comput. Vis., Imag. Comput. Graph. Theory Appl. (VISIGRAPP)*, 2017, pp. 96–101.
- [77] J. Sayahzadeh, H. Pourreza, and J. S. Fadardi, "A fast, robust, automatic blink detector," *Iranian J. Med. Phys.*, vol. 11, no. 4, pp. 334–349, 2014.
- [78] R. W. Schafer, "What is a Savitzky-Golay filter? [Lecture notes]," *IEEE Signal Process. Mag.*, vol. 28, no. 4, pp. 111–117, Jul. 2011.
- [79] F. Scholkmann, F. Scholkmann, S. Kleiser, A. J. Metz, R. Zimmermann, J. M. Pavia, U. Wolf, and M. Wolf, "A review on continuous wave functional near-infrared spectroscopy and imaging instrumentation and methodology," *NeuroImage*, vol. 85, no. 1, pp. 6–27, Jan. 2014.
- [80] W. Sewell and O. Komogortsev, "Real-time eye gaze tracking with an unmodified commodity webcam employing a neural network," in *Proc. Extended Abstr. Hum. Factors Comput. Syst. (CHI)*, 2010, pp. 3739–3744.
- [81] F. A. P. Sharma and S. B. Y. Jobanputra, "Augmentative and assistive communication in patients of locked-in syndrome: A case report," in *Replace, Repair, Restore, Relieve—Bridging Clinical and Engineering Solutions in Neurorehabilitation* (Biosystems & Biorobotics), vol. 7, W. Jensen, O. Andersen, and M. Akay, Eds. Cham, Switzerland: Springer, 2014.
- [82] E. Smith and M. Delargy, "Locked-in syndrome," *Bmj*, vol. 330, no. 7488, pp. 406–409, 2005.
- [83] T. Soukupová, "Real-time eye blink detection using facial landmarks," in *Proc. 21st Comput. Vis. Winter Workshop Luka Cehovin, R. Mandeljc and V. Štruc*, Eds. Slovenia: Rimske Toplice, Feb. 2016.
- [84] E. M. Spinelli, N. H. Martinez, and M. A. Mayosky, "A single supply biopotential amplifier," *Med. Eng. Phys.*, vol. 23, no. 3, pp. 235–238, 2001.
- [85] K. Suefusa and T. Tanaka, "A comparison study of visually stimulated brain-computer and eye-tracking interfaces," *J. Neural Eng.*, vol. 14, no. 3, 2017, Art. no. 036009.
- [86] Y. Sun, S. Zafeiriou, and M. Pantic, "A hybrid system for on-line blink detection," in *Proc. Hawaii Int. Conf. Syst. Sci.*, 2013, pp. 1–5.
- [87] A. Tharwat, "Classification assessment methods," *Appl. Comput. Inform.*, 2018. [Online]. Available: <http://www.sciencedirect.com/science/article/pii/S2210832718301546>. doi: 10.1016/j.aci.2018.08.003.
- [88] R. Valenti and T. Gevers, "Accurate eye center location and tracking using isophote curvature," in *Proc. IEEE Conf. Comput. Vis. Pattern Recognit. (CVPR)*, Jun. 2008, pp. 1–8.
- [89] M. G. V. Koningsbruggen, M. V. Peelen, E. Davies, and R. D. Rafal, "Neural control of voluntary eye closure: A case study and an fMRI investigation of blinking and winking," *Behav. Neurol.*, vol. 25, no. 2, pp. 103–109, 2012.
- [90] B. B. Velichkovsky, M. A. Rumyantsev, and M. A. Morozov, "New solution to the midas touch problem: Identification of visual commands via extraction of focal fixations," *Procedia Comput. Sci.*, vol. 39, pp. 75–82, Jan. 2014.
- [91] S. Venkataramanan, P. Prabhat, S. R. Choudhury, H. B. Nemade, and J. Sahambi, "Biomedical instrumentation based on electrooculogram (EOG) signal processing and application to a hospital alarm system," in *Proc. Int. Conf. Intell. Sens. Inf. Process.*, Jan. 2005, pp. 535–540.
- [92] P. Viola and M. Jones, "Rapid object detection using a boosted cascade of simple features," in *Proc. IEEE Comput. Soc. Conf. Comput. Vis. Pattern Recognit. (CVPR)*, vol. 1, Dec. 2001, pp. 511–518.
- [93] K. Wang and Q. Ji, "Real time eye gaze tracking with Kinect," in *Proc. 23rd Int. Conf. Pattern Recognit. (ICPR)*, Dec. 2016, pp. 2752–2757.
- [94] C. Weiss and J. F. Disterhoft, "Evoking blinks with natural stimulation and detecting them with a noninvasive optical device: A simple, inexpensive method for use with freely moving animals," *J. Neurosci. Methods*, vol. 173, no. 1, pp. 108–113, 2008.
- [95] L. C. Wijesekera and P. N. Leigh, "Amyotrophic lateral sclerosis," *Orphanet J. Rare Diseases*, vol. 4, no. 1, p. 3, 2009.
- [96] J. Wolpaw, N. Birbaumer, W. J. Heetderks, D. J. McFarland, P. H. Peckham, G. Schalk, E. Donchin, L. A. Quatrano, C. J. Robinson, and T. M. Vaughan, "Brain-computer interface technology: A review of the first international meeting," *IEEE Trans. Rehabil. Eng.*, vol. 8, no. 2, pp. 164–173, Feb. 2000.
- [97] X. Xiong and F. De La Torre, "Supervised descent method and its applications to face alignment," in *Proc. IEEE Conf. Comput. Vis. Pattern Recognit. (CVPR)*, Jun. 2013, pp. 532–539.
- [98] S. Zarei, K. Carr, L. Reiley, K. Diaz, O. Guerra, P. F. Altamirano, W. Pagani, D. Lodin, G. Orozco, and A. Chinae, "A comprehensive review of amyotrophic lateral sclerosis," *Surg. Neurol. Int.*, vol. 6, p. 171, Nov. 2015.
- [99] X. Zheng, X. Li, J. Liu, W. Chen, and Y. Hao, "A portable wireless eye movement-controlled human-computer interface for the disabled," in *Proc. Int. Conf. Complex Med. Eng. (ICME)*, Tempe, AZ, USA, Apr. 2009, pp. 1–5.
- [100] L. Zoubek, S. Charbonnier, S. Lesecq, A. Buguet, and F. Chapotot, "Feature selection for sleep/wake stages classification using data driven methods," *Biomed. Signal Process. Control*, vol. 2, no. 3, pp. 171–179, 2007.



devices or techniques for helping people to access a computer.

**ALBERTO J. MOLINA-CANTERO** was born in Lucena, Córdoba, in 1967. He received the B.S. degree in physics with intensification in electronics, in Seville, in 1990, and the Ph.D. degree from the Universidad de Sevilla, in 2010, where he has been a Professor, since 1990. He has authored five books and more than 30 research papers, holds three inventions, and took part in more than 10 projects. His research interests include signal processing, sensors, and the development of new



**CLARA LEBRATO-VÁZQUEZ** was born in Seville, Spain, in 1993. She received the B.Sc. degree in health engineering and the M.Sc. in water engineering from the Universidad de Sevilla, in 2015. She has been an author of two peer-reviewed journal publications and her work has been presented at several international conferences. Her wide research interests include bacterial growth in titanium prosthetics to the development and testing of sensors and interfaces for computer accessibility.



**MANUEL MERINO-MONGE** was born in Seville, Spain, in 1983. He received the master's degree in computer engineering from the Universidad de Sevilla, in 2010, where he received the Ph.D. degree from the TAIS (Technologies for Care, Inclusion and Health) Research Group, in 2015. His research interests include biomedical signal processing, affective computing, human computer interface, augmentative and alternative communication, and assistive technology.



**ROYLÁN QUESADA-TABARES** was born in Artemisa, La Habana, in 1990. He received the degree in telecommunications and electronics engineering in Havana, in 2014, and the master's degree in computers and networks from the Universidad de Sevilla, in 2016, where he is currently pursuing the Ph.D. degree. His research interests include machine learning, sensors, signal processing, and human computer interfaces.



**JUAN A. CASTRO-GARCÍA** was born in Lora del Río, Seville, in 1986. He received the master's degree in computers and networks engineering from the Universidad de Sevilla, in 2011. He is currently a Professor and a Ph.D. student associated to the Department of Electronic Technology. His research interests include signal processing, sensors, and human computer interfaces.



**ISABEL M. GÓMEZ-GONZÁLEZ** has been a Senior Researcher and a full time Ph.D. Lecturer with the Electronic Technology Department, Universidad de Sevilla, since 1990. Her teaching is centered on digital electronic and biomedical technology disciplines in bachelor degree and computer science in master degree. She has directed numerous final career projects about the design and implementation of serious games and toys adaptation in order to improve the cognitive and motor skills of adults and children with cerebral palsy. She is the Head of TAIS (Technologies for Care, Inclusion and Health) Research Group, where she has been managing several Ph.D. thesis and national research projects related to human computer interfaces, biosignal processing, and ambient assisted living.

...